Development of experimental methodology for evaluation of rubber-steel ahesion at fatigue loading conditions

Bc. Ondřej Kotula

Master's thesis

2017

Tomas Bata University in Zlín
Faculty of Technology

Univerzita Tomáše Bati ve Zlíně
Fakulta technologická
Ústav inženýrství polymerů
akademický rok: 2016/2017

ZADÁNÍ DIPLOMOVÉ PRÁCE
(PROJEKTU, UMĚLECKÉHO DÍLA, UMĚLECKÉHO VÝKONU)

Jméno a příjmení:	**Bc. Ondřej Kotula**
Osobní číslo:	**T15262**
Studijní program:	**N2808 Chemie a technologie materiálů**
Studijní obor:	**Inženýrství polymerů**
Forma studia:	**prezenční**
Téma práce:	**Vývoj experimentální metodiky stanovení adheze pryž-ocel při dynamickém únavovém zatěžování.**

Zásady pro vypracování:

1. Literární rešerše adheze pryž-ocel při kvazi-statickém i dynamickém zatěžování pryže založených na různých gumárenských směsích.
2. Návrh měřící metodiky analýzy adheze pryž-ocel při dynamickém zatěžování s on-line charakterizací rychlosti separace obou komponentů.
3. Sestavení teoretického základu pro měřící metodologii.
4. Konstrukce upínacích čelistí použitelných pro stávající zkušební stroje.
5. Výroba gumárenských směsí na základě příkladové receptury používané pro výrobu nárazníkových směsí.
6. Vulkanizace zkušebních těles.
7. Provedení experimentálního měření.
8. Vyhodnocení naměřených dat.
9. FEM analýza reálné části pryž-ocel s využitím získaných dat.
10. Vypracovaní textové části diplomové práce.

Rozsah diplomové práce:

Rozsah příloh:

Forma zpracování diplomové práce: **tištěná/elektronická**

Seznam odborné literatury:

[1] OZAWA, Kenichi a Kazuhiko MASE. Evidence for chemical bond formation at rubber-brass interface: Photoelectron spectroscopy study of bonding interaction between copper sulfide and model molecules of natural rubber. Surface Science. 2016, 2016(654), 14-19.

[2] ŠŮLA, Miroslav. Pojení pryže s kovem. Zlín: ČSPCH. 2007. 63 s. ISBN 978-80-02-01934-3

[3] CROWTHER, Bryan.: The Handbook of Rubber Bonding. Rapra technology LTD. United Kingdom, 2001. 3-97 s. ISDN 1-85957-394-0.

Vedoucí diplomové práce: **Ing. Radek Stoček, Dr.**
Ústav inženýrství polymerů

Datum zadání diplomové práce: **2. ledna 2017**

Termín odevzdání diplomové práce: **10. května 2017**

Ve Zlíně dne 1. března 2017

UNIVERZITA TOMÁŠE BATI VE ZLÍNĚ
Fakulta technologická
L.S.

doc. Ing. František Buňka, Ph.D.
děkan

doc. Ing. Tomáš Sedláček, Ph.D.
ředitel ústavu

Příjmení a jméno: Kotula Ondřej Obor: Inženýrství polymerů

P R O H L Á Š E N Í

Prohlašuji, že

- beru na vědomí, že odevzdáním diplomové/bakalářské práce souhlasím se zveřejněním své práce podle zákona č. 111/1998 Sb. o vysokých školách a o změně a doplnění dalších zákonů (zákon o vysokých školách), ve znění pozdějších právních předpisů, bez ohledu na výsledek obhajoby[1)];
- beru na vědomí, že diplomová/bakalářská práce bude uložena v elektronické podobě v univerzitním informačním systému dostupná k nahlédnutí, že jeden výtisk diplomové/bakalářské práce bude uložen na příslušném ústavu Fakulty technologické UTB ve Zlíně a jeden výtisk bude uložen u vedoucího práce;
- byl/a jsem seznámen/a s tím, že na moji diplomovou/bakalářskou práci se plně vztahuje zákon č. 121/2000 Sb. o právu autorském, o právech souvisejících s právem autorským a o změně některých zákonů (autorský zákon) ve znění pozdějších právních předpisů, zejm. § 35 odst. 3 [2)];
- beru na vědomí, že podle § 60 [3)]odst. 1 autorského zákona má UTB ve Zlíně právo na uzavření licenční smlouvy o užití školního díla v rozsahu § 12 odst. 4 autorského zákona;
- beru na vědomí, že podle § 60 [3)]odst. 2 a 3 mohu užít své dílo – diplomovou/bakalářskou práci nebo poskytnout licenci k jejímu využití jen s předchozím písemným souhlasem Univerzity Tomáše Bati ve Zlíně, která je oprávněna v takovém případě ode mne požadovat přiměřený příspěvek na úhradu nákladů, které byly Univerzitou Tomáše Bati ve Zlíně na vytvoření díla vynaloženy (až do jejich skutečné výše);
- beru na vědomí, že pokud bylo k vypracování diplomové/bakalářské práce využito softwaru poskytnutého Univerzitou Tomáše Bati ve Zlíně nebo jinými subjekty pouze ke studijním a výzkumným účelům (tedy pouze k nekomerčnímu využití), nelze výsledky diplomové/bakalářské práce využít ke komerčním účelům;
- beru na vědomí, že pokud je výstupem diplomové/bakalářské práce jakýkoliv softwarový produkt, považují se za součást práce rovněž i zdrojové kódy, popř. soubory, ze kterých se projekt skládá. Neodevzdání této součásti může být důvodem k neobhájení práce.

Ve Zlíně ……

……

[1)] zákon č. 111/1998 Sb. o vysokých školách a o změně a doplnění dalších zákonů (zákon o vysokých školách), ve znění pozdějších právních předpisů, § 47 Zveřejňování závěrečných prací:

(1) Vysoká škola nevýdělečně zveřejňuje disertační, diplomové, bakalářské a rigorózní práce, u kterých proběhla obhajoba, včetně posudků oponentů a výsledku obhajoby prostřednictvím databáze kvalifikačních prací, kterou spravuje. Způsob zveřejnění stanoví vnitřní předpis vysoké školy.

(2) Disertační, diplomové, bakalářské a rigorózní práce odevzdané uchazečem k obhajobě musí být též nejméně pět pracovních dnů před konáním obhajoby zveřejněny k nahlížení veřejnosti v místě určeném vnitřním předpisem vysoké školy nebo není-li tak určeno, v místě pracoviště vysoké školy, kde se má konat obhajoba práce. Každý si může ze zveřejněné práce pořizovat na své náklady výpisy, opisy nebo rozmnoženiny.

(3) Platí, že odevzdáním práce autor souhlasí se zveřejněním své práce podle tohoto zákona, bez ohledu na výsledek obhajoby.

[2] zákon č. 121/2000 Sb. o právu autorském, o právech souvisejících s právem autorským a o změně některých zákonů (autorský zákon) ve znění pozdějších právních předpisů, § 35 odst. 3:

(3) Do práva autorského také nezasahuje škola nebo školské či vzdělávací zařízení, užije-li nikoli za účelem přímého nebo nepřímého hospodářského nebo obchodního prospěchu k výuce nebo k vlastní potřebě dílo vytvořené žákem nebo studentem ke splnění školních nebo studijních povinností vyplývajících z jeho právního vztahu ke škole nebo školskému či vzdělávacího zařízení (školní dílo).

[3] zákon č. 121/2000 Sb. o právu autorském, o právech souvisejících s právem autorským a o změně některých zákonů (autorský zákon) ve znění pozdějších právních předpisů, § 60 Školní dílo:

(1) Škola nebo školské či vzdělávací zařízení mají za obvyklých podmínek právo na uzavření licenční smlouvy o užití školního díla (§ 35 odst. 3). Odpírá-li autor takového díla udělit svolení bez vážného důvodu, mohou se tyto osoby domáhat nahrazení chybějícího projevu jeho vůle u soudu. Ustanovení § 35 odst. 3 zůstává nedotčeno.

(2) Není-li sjednáno jinak, může autor školního díla své dílo užít či poskytnout jinému licenci, není-li to v rozporu s oprávněnými zájmy školy nebo školského či vzdělávacího zařízení.

(3) Škola nebo školské či vzdělávací zařízení jsou oprávněny požadovat, aby jim autor školního díla z výdělku jím dosaženého v souvislosti s užitím díla či poskytnutím licence podle odstavce 2 přiměřeně přispěl na úhradu nákladů, které na vytvoření díla vynaložily, a to podle okolností až do jejich skutečné výše; přitom se přihlédne k výši výdělku dosaženého školou nebo školským či vzdělávacím zařízením z užití školního díla podle odstavce 1.

ABSTRAKT

V teoretické části je práce zaměřená na nejdůležitější aspekty při tvorbě nového spojení, zejména mezi gumou a ocelí a to včetně metod povrchových úprav, stručného seznamu významných adheziv přes popis samotného spoje až po jeho testování. Experiment je zaměřen na popis jednotlivých kroků při tvorbě spoje v laboratorních podmínkách a především na samotné zkušební metody a jejich význam při hodnocení kvality spoje se zvláštním ohledem na dynamické namáhání.

Klíčová slova: metodika, adheze, dynamické zkoušky, spojení, gumokovové výrobky

ABSTRACT

In the theoretical part, the thesis is focused on the most important aspects in the creation of a new adhesive connection, especially between rubber and steel, including surface treatment methods, a short list of important adhesives through the description of the bond itself and its testing. The analysis focuses on the description of the individual steps in the creation of the bond in the laboratory conditions and primarily on the test methods and their importance in evaluating the quality of the connection with the special regards on the fatigue loading conditions.

Keywords: methodology, adhesion, dynamic tests, bonding, rubber-metal products

Acknowledgement

My first thanks belongs to Ing. Radek Stoček Ph.D. who introduced me to the problematics, inspired me greatly in learning new approaches and above all showed wonderful patience. To Mubea company for the support. To my family for giving me the opportunity to study. To TBU's Faculty of Technology. And also to my brain for not letting me down, when I needed him most.

„Get your facts first, then you can distort them as you please."

Mark Twain

Prohlašuji, že odevzdaná verze diplomové práce a verze elektronická nahraná do IS/STAG jsou totožné.

CONTENTS

INTRODUCTION **9**
I THEORY **10**
1 SURFACE PREPARATION **11**
1.1 MECHANICAL METHODS 11
1.1.1 Initial degreasing 11
1.1.2 Alkaline removal 12
1.1.3 Grinding 12
1.1.4 Blasting 13
1.2 CHEMICAL METHODS 14
1.2.1 Parkerizing 14
1.2.2 Galvanizing 15
2 BONDING AGENTS **17**
2.1 HARDENED RUBBER 17
2.2 HALOGENATED RUBBER 17
2.3 POLYURETHANES 18
2.4 EPOXIDES 19
2.5 CYANOACRYLATES 20
3 BONDING THE MATERIALS **21**
3.1 FUNDAMENTAL CONCEPT OF ADHESION 21
3.2 MOLDED RUBBER INTO METAL PART 21
3.3 RUBBER-METAL BOND REQUIREMENTS 22
3.4 MECHANICAL LINKAGE 22
3.4.1 Structure of mechanical connection 22
3.5 GLUING 23
3.5.1 Structure of glued bond 24
3.6 VULCANIZATION 26
3.6.1 Structure of cured bond 26
4 OTHER BENEFITIAL TESTS **28**
4.1 FILLERS EXAMINATION 28
4.2 BASIC ABRASION TEST 30
II ANALYSIS **31**
5 SAMPLE PREPARATION **32**
5.1 COMPOUNDATION 32
5.2 VULCANIZATION CHARACTERISTICS 32
5.3 PRESSURE MOLDING 34
6 TESTING **35**
6.1 QUASISTATIC TESTS 35
6.1.1 Simple tensile test 35
6.1.2 Shear test 38
6.1.3 Peel test 40

6.2 DYNAMIC TEST 43
6.2.1 Hysteresis 43
6.2.2 Fatigue peel test 46
6.3 FEM ANALYSIS 52
CONCLUSION 55
BIBLIOGRAPHY 57
LIST OF ABBREVIATIONS 61
LIST OF FIGURES 65
LIST OF TABLES 67

INTRODUCTION

For the benefits of future research an update of methodology is considered to simplify, yet extend present ways when testing rubber-steel adhesion.

In most cases, tests under mass production conditions are simplified to find out fundamental description that is often considered sufficient. Although such methods carry the basic information, they often provide a insufficient data volume needed for further analysis.

For better understanding of the phenomena occurred when loading particular system, it is necessary to use modern imaging and testing techniques. Elastomers and their related products are used very often in the automotive sector and detailed analysis can help to explain how implement such materials as efficiently as possible. In the case of a moving car, think of it always as a dynamic process, therefore the simulation of dynamic processes that can be decisive in correctly identifying specific means to use discussed materials.

Nowadays, a number of corporations are inspiring advances in science and expanding into various science problematics. The field of polymer sciences is still very lucrative, especially concerning elastomers, and new knowledge is gaining momentum that is slowly pushing mankind towards the understanding of this world.

I. THEORY

1 SURFACE PREPARATION

All surface treating methods are reliant to material on which they are performed. Before connecting metal workpiece to rubber a removal of all the impurities and dirt pieces is essential. A dust particle is considered a mechanical impurity as well as grease and other residue. Every product of a chemical reaction (surface oxidation, for example) result in chemical impurity. Each of these impurities requires a specific approach when a proper surface treatment method is selected. [1]

1.1 Mechanical methods

Often the metals come from foundry and other shops coated with oil and significant layer of oxide on the exposed surfaces. Oxides may develop further during storage or of course during lifetime of the product. All the unwanted materials must therefore be removed. The oil, hidden in cavities may evaporate and expand during vulcanization. Oxides bring other inconvenience. Bond between the metal surface and the oxide is very often considerably weaker than cohesion in metal, so their presence cause adhesive force to fail. All metals create a fresh layer of oxide immediately after treating, so rapid degreasing and application of primer, adhesive or other coating is needed. [2]

1.1.1 Initial degreasing

Degreasing is the very first step to create firm and quality connection between any materials, so the methods are widely used in any form. Insufficient process ends up in defects on the bonded interface, which eventually leads to faulty product. [2] The importance of degreasing is demonstrated on the graphic image below.

Figure 1 – Example of degreasing effect [3]

Most common method is removal by vapor of a chlorinated solvent (trichloroethylene, propyl alcohol, perchlorethylene e.g.) which must be of neutral pH otherwise a further corrosion is initiated. Metal must remain in the solvent vapor for such time as the material reaches the temperature. This means the condensation process ceased to continue. Environmental impact is of course a very noticeable and popular issue, so the solvent must be used exclusively indoors and various regulations on the safety, equipment and waste disposal are in force. [2]

1.1.2 Alkaline removal

This has been an alternative method to initial processes, used in dip tub or spray set. Process efficiency depends on the strength of alkaline, the temperature and of course time of exposure which can be set up to two hours, as regards the amount of grease. Dip tanks need to be followed by water tanks to remove the alkaline. [2]

Solvent dip tanks are the most common in large scale degreasing and are very expansive to run. For the maximum efficiency a number of tanks is set in to completely remove impurities. This method is not suitable for small scale production or products. [2]

1.1.3 Grinding

Listed procedures are based on removing thin surface layers or converting them via plastic deformation, so these practices find use when the specific proportions of the product are not relevant. In other way this may also prove a useful feature for finishing the product into exact diameter, when no other treating is required. [4]

The primary purpose is progressive material removal, thus removing coarse roughness. Procedure operates with grinding belts or discs with fixed or loose coupling to abrasive. Inequality of the surface decides on which grade of roughness will be used. Very rough grinding proceeds at dry conditions availing abrasive material with the grain size of 24 to 200. A fine grinding (smoothing) works with the grain size of 120 to 240 but an addition of lubricant is used to lower friction and prevent overheating. There is no exact boundary between grinding and polishing. [4]

Grain size is determined according to sieve density, where higher number gives finer abrasive. [4]

No exact border exists between grinding and polishing as far as tools are considered. There's a less material removal while the surface layer undergoes a plastic deformation which even

the slightest bumps and inequalities. Polishing can be performed on basic material as well as on the surface finishing yet done (galvanized coatings). Quality of the surface modifications are based on peripheral speed of the tool and the polishing paste used. The paste apart from lipid components contains a large variety of abrasives such as chromium oxide, ferric oxide, alumina, calcium oxide or pumice. While pre-polishing a sharpest paste and harder fabric or leather discs are used. Final polishing is performed with very soft, slow moving disc and drier and smoother paste. Along with grinding these methods are the most costly. [4]

1.1.4 Blasting

The main purpose is to clean the surface from corrosive elements, oxides at most and achieve specific level of roughness. While blasting a high velocity particles of blasting material pound the surface. Effectivity relies on type of the abrasive, the grain size, applied pressure, diameter, angle and distance of the nozzle. [2, 4]

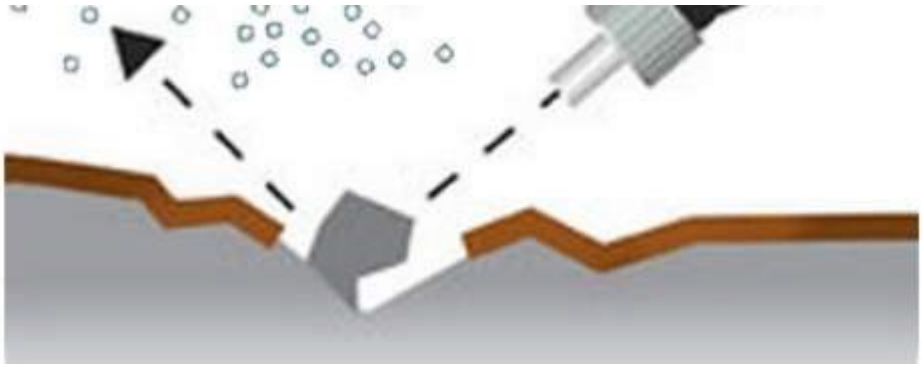

Figure 2 – Approximate demonstration of blasting mechanism [5]

The most general blasting materials are [3, 6]:

- cast iron grit (high removal capability and durability, economical and hygienic)
- silica sand (cheap, low removal capability, shatters and may cause silicosis)
- chopped wire (the most durable, does not shatter, 5 times the price of cast iron grit)
- specials (plastic material grit, glass pellets, ideal for smoothing)
- abrasives (silicon carbide, alumina, like silica sand, but more durable)

Blasting is defined by number of specifics. Main impact lies in material (mass, hardness, size, shape), its velocity and areal density of landed particles over time. Process time is an effective specific also. Sharper and harder particles, according to landing angle separate splinters of the material while derusting and cleaning the surface which is accordingly roughened.

Very hard material also creates cavities or the debris may stuck in the surface layers of blasted element. If the landing particles are soft shaped or round, surface forms via plastic deformation and the finished surface has dented character. This is ideal for metals and polymers. Plastic deformation of the surface also provides improvement in surface toughness. [2, 4]

1.2 Chemical methods

In general, all such methods are based on chemical reaction between reagent and surface of the material. Every material however is very specific in chemical reactivity, so the choice of a correct agent is far more crucial. Quality of the treated surface may occur variable if the process is not controlled correctly. The most suitable mixtures for the job are nitric, sulphuric, chromic and hydrofluoric acid. [2]

Concerning stainless steel, there are various systems suitable for pre-treating, often including strong acids that disrupt crystal grain boundaries giving roughness to the steel which enhances specific area and the adhesion. [2]

1.2.1 Parkerizing

One of the best means to chemically treat steel, also suitable for zinc, aluminum, magnesium and alloys. Other than surface preparation this method is vastly used as finishing, especially in the firearms industry for. Parkerizing, also known as phosphate coating rests in immersing a metal element in phosphating solution. Specifics of the exact technique depend on nature of the phosphating solution. During the process a very thin layer (up to 2 microns) of the metal phosphate (zinc or manganese e.g.) is created upon the surface providing excellent protection against corrosion. [2, 7]

For preparation of the steel surface when bonding, a zinc dihydrogen phosphate in mixture with phosphoric acid is a very common solution with pH value under 7. Nitric acid may be used as catalyst. The character of the deposit depends on the microstructure of the steel and the underlying crystal lattice. Having martensitic structure a surface will support phosphate in form of fine flake while cold rolled steel with different structure orientation rises for lumpy large flake which under stress is easily broken apart. [2]

Especially for waterborne systems a phosphate, modified by calcium shows better results when re-infecting the metal surface than conventional grit blasting. [8]

Although used for years now a process control can be difficult. Variability in thickness of phosphate deposit causes issues. When too thick, phosphate lacks cohesion integrity and becomes friable which ends up in failure under load. Moderate or thin layers often require additional passivation of the uncovered or even minimally covered areas. To passivate a treating with chromic acid forms chromium oxide, however a chromium oxide won't react with bonding agents readily thus is more suitable for finishing. [2]

Figure 3 – Phosphate coating setup [9]

1.2.2 Galvanizing

For the wide use of zinc this method is also called zinc coating, covering the surface in brass is known as brass plating. Maximum effect is achieved when the coating is hot dipped onto the cleaned metal giving a galvanized finish. Bonding may occur difficult when the crystalline stricture of the galvanized metal starts to flake off under load resulting in fracture. [2]

There are some recommendations for cleaning and zinc coating [10]:

- Degreasing the metal part
- Abrasion of the galvanized surface with grit
- Degreasing then applying the adhesive ASAP

Or the more widely spread method [10]:

- Degreasing the metal part

- Immersion in a solution (20 parts by weight) of concentrated hydrochloric acid with (80 parts by weight) de-ionized water. 2 – 4 minutes at 25 °C
- Thorough flash out in cold, running, de-ionized water
- Drying in oven. 20 – 30 minutes at 70 °C
- Applying the adhesive ASAP

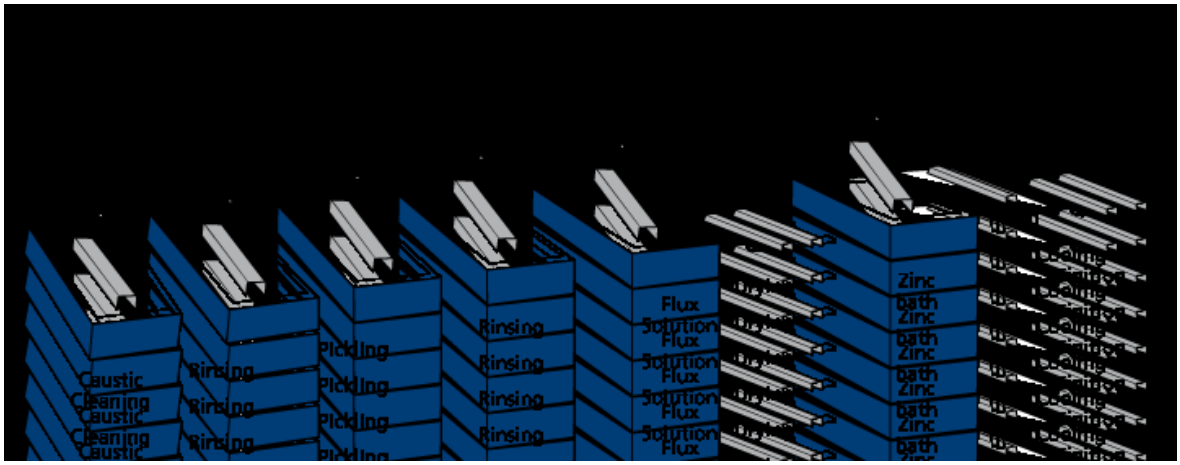

Figure 4 – Zinc coating procedure demonstration [11]

2 BONDING AGENTS

Bonding agent creates an interlayer between the metal and the rubber part. As for today, trends head for maximal compatibility of coupling systems with appropriate materials.

The most common agent is [1]:

- Hardened rubber
- Halogenated rubber
- Polyurethanes
- Epoxides
- Cyanoacrylates

Variety of the adhesives in production is too comprehensive to be discussed in specific details. Overall review on the issue is better composed in mentioned literature. [12]

2.1 Hardened rubber

Already outdated system, originating in the 19th century provides a vulcanized connections. On the treated surface a layer of rubber is applied. This mixture contents 25 – 47 phr in uncured state either in form of foil or rubber cement. Thus prepared specimen is then heated in autoclave. [1]

Main drawback of such manner lie in loss of mechanical properties above 70°C when the bonding rubber becomes soft and fragile. At present, the method has been replaced mostly by utilizing halogenated rubbers. However is still rarely being used. [1]

2.2 Halogenated rubber

Predominantly chlorinated rubbers, treated with chlorine or hydrogen chloride in form of rubber solution, which is blended with pure rubber and solvents to create a viscous system. Thus prepared solution is easy to manipulate with and can be used in spraying, brushing etc. Nowadays a wide range of options is available on the market, from solution, contact adhesive, sealant to tape. [1]

Halogenated rubber, mostly derived from butyl rubber (IIR) shows the best gas impermeability from all rubber spectrum. This feature is often used in tire production industry, where halogenated IIR forms inner layer of tire. Most significant advantages include a fine quality of the final bond, high chemical and outdoor resistance, increased storage time and chemical

similarity to polar materials. In case of bonding nonpolar rubber a medium-polar interlayer is necessary. [1, 15,14]

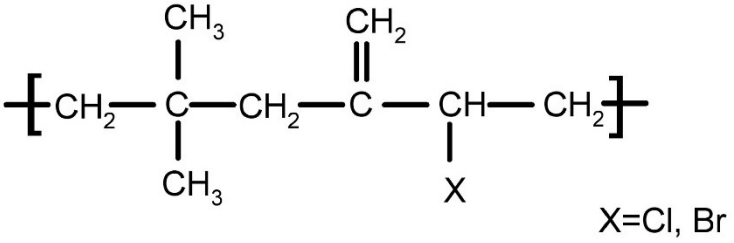

Figure 5 – Example of IIR monomer unit [12]

2.3 Polyurethanes

Isocyanates and polyalcohols create highly reactive mixture which at certain circumstances leads to polyurethane ever since 1937, when Bayer et al. pioneered the first reaction. Addition polymer is formed swiftly at very mild conditions (atmospheric pressure, room temperature). Polyurethanes (PUR) are considered the most versatile of all chemical compounds. Adhesives sure, but sealants, soft and hard foam, or elastomers, those are all PUR forms. [12]

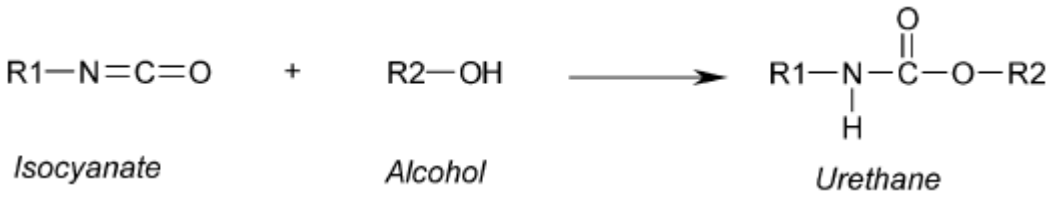

Figure 6 – Chemical reaction resulting in monomer [12]

Reactivity of the end groups is dependent on the chemical character, listed below (Table 1) Final polymer exceeds in mechanical properties, especially at high shear strength. Created links are very tough and durable at low temperatures and fatigue loading conditions. The upper operating temperature ranges around 120°C. Polyurethane is water soluble therefore may react sensitively to moisture as well as its starting reagents, so the range of application is considerably limited. On the other hand, resistance to non-polar substance sis excellent. Adhesives are produced in 1K or 2K form. While single component results its reaction in elastomer, double component adhesive reacts in polyadition, creating firm thermoset. [12]

Table 1 – Reactivity degree of the end groups in PUR [12]

Hydrogen compound	Formula	Reactivity degree
Primary aliphatic amine	$R-NH_2$	Highly reactive
Secondary aliphatic amine	R_2-NH	↓
Primary aromatic amine	$Ar-NH_2$	
Primary hydroxyl	$R-CH_2-OH$	
Secondary hydroxyl	$R_2-CH-OH$	
Tertiary hydroxyl	R_3-C-OH	
Phenol	$Ar-OH$	Less reactive
Water	$H-O-H$	

2.4 Epoxides

Ideal for vulcanization processes epoxides are possibly the very best of bonding agents. Low MW, high viscosity liquid in blend with other additives creates chemically resistant, thermally stable resin with excellent mechanical properties. On the other hand, final resin due to high degree of crosslinking may behave fragile with low impact strength. Polymer exhibits superior adhesion to metals and other polar materials. [2]

Currently there are several of epoxy resin in production: [12]

- Pure epoxy resins
- Epoxy – phenolic resins
- Epoxy – silicone resins

The eldest and still common is bifunctional diglycid ether of bisphenol A (Fig. 6), multifunctional with three or four epoxy groups shows great adhesion and mechanical properties and glass transition temperature up to 300 °C. [12]

1K epoxy forms into thermoset during thermo-initiated polyadition and is used widely across the industry as a structural glue. 2K resins require greater care while mixing components, the exact ratio and workability time are crucial factors while using 2K glues. However certain combinations of 2K can be used as a no mix system. [12]

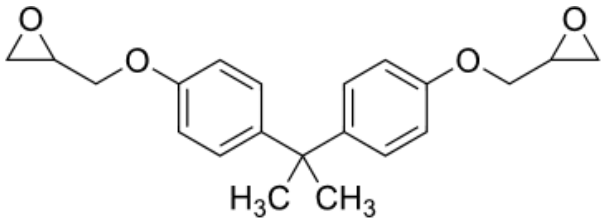

Figure 7 – Diglycid ether of bisphenol A [15]

2.5 Cyanoacrylates

The main application for cyanoacrylate adhesives are in domestic use and wide range of industrial manufacture (plastics, electronics, shoes, etc.). Development of the fingerprint is also a specific feature of certain cyanoacrylate. Most adhesives are delivered in form of transparent liquid with moderate to low surface energy and largely variable viscosity and show no toxicity to humans. [16]

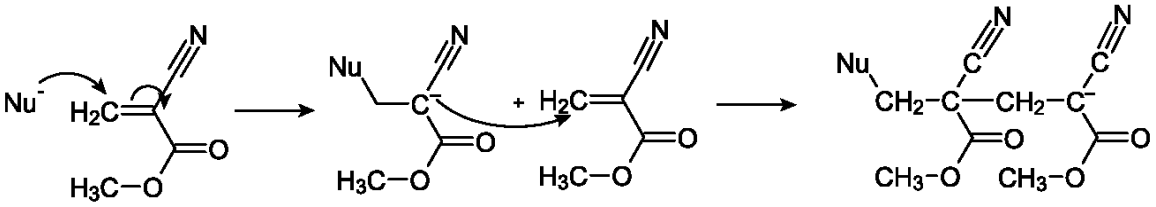

Figure 8 – polymerization of methyl-2-cyanoacrylate [17]

The end group (methyl on Fig. 8) is the determining factor of the mechanical properties of the final bond. Methyl cyanoacrylate is considered least toxic therefore suitable for wound closure in medical application. [18]

Acrylate deposit forms a thermoplastic polymer which reaction is initiated mostly due to air humidity. However larger humidity or direct moisture exposure cause polymer chains to crack. Most producers offer vast variety of modded adhesives suitable for any way of use from flexible to high strength, temperature. Time to reach handling strength is the most beneficial factor. [16, 18]

3 BONDING THE MATERIALS

3.1 Fundamental concept of adhesion

Adhesion is often defined as the attraction between dissimilar components for one another. According to standard ASTM D907 – 15 "The state in which two surfaces ate held together by interfacial forces which may consist of valence forces or interlocking action or both." In reality one must consider the difference between *basic* adhesion, summering all interfacial and intermolecular forces and *practical* adhesion, which is often described as force or work, needed to disrupt the bond. Currently there are four basic types of material failure, all of which figured below. [9, 19]

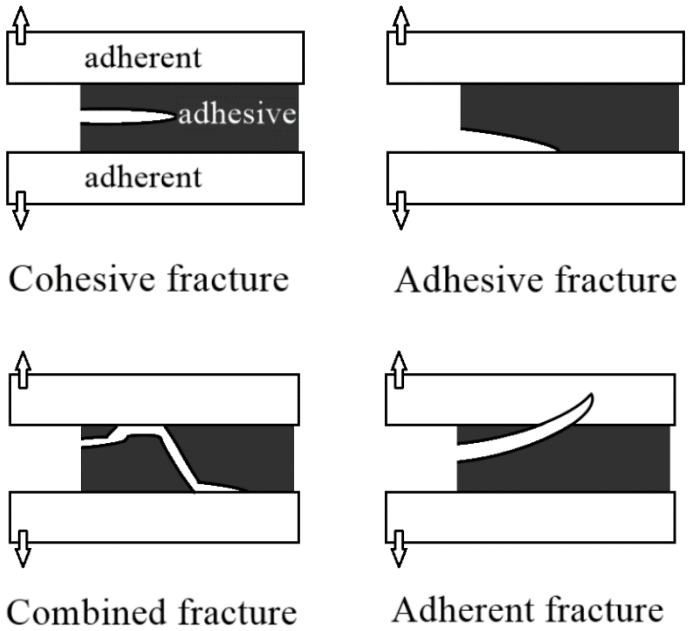

Figure 9 – Basic type of fracture

3.2 Molded rubber into metal part

The metal part serves as reinforcement of the final product. All physical and mechanical properties are significantly different from pure rubber component. Metal part's function is to transfer the applied force to the rubber part. Today's most common, economical and suitable metal is steel. The higher the quality the more challenging requirements for surface treating are. [1]

3.3 Rubber-metal bond requirements

Due to material characteristics, expectations are often very high and specific: [1]

- bond strength is equal or higher than the strength of rubber,
- bond is resistant to mechanical degradation,
- bond is resistant to chemical degradation,
- bond is resistant to thermal degradation and photo degradation,
- final product must not burden on the environment,
- disposal of the products must not pollute the environment

3.4 Mechanical linkage

In production of mechanical links the single parts are assembled in one piece which is achieved combining the metal and the rubber without presence of any chemical agent. For anchorage a sufficient friction between the materials is required. Consistency and functionality of the connection thus entirely depends on the structural design, therefore preparation processes of the single parts. Usually the rubber component is attached to the metal part or the press molded element is mounted between two reinforcing rubber parts. In last case, a rubber knob holds the other elements together. [1]

3.4.1 Structure of mechanical connection

The demonstration (Fig. 10) shows an example of mechanical linkage, represented by the macromolecules of rubber, settled in surface dents or cavities of the steel substrate. Attachment is possible due to non-covalent bonding. Mechanical lock contributes on the final strength in every final product but its effect fades as the chemical bonds between adhesive and adherent are being created. Such connection is suitable in case of dismountable products. [20]

However if intimate contact is not sufficient, roughness leads to decrease in adhesion by producing uncoated voids. Concerns were raised about general validity of mechanical adhesion mechanism. Often a mechanical abrasion cause micro radicals to develop and act furthermore as reactive components. [10]

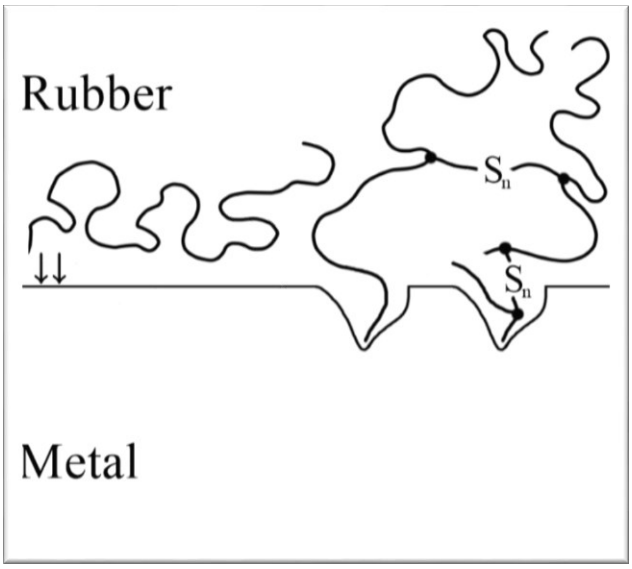

Figure 10 – Approximate mechanical adhesion

This type is inducted partly while attaching the materials, the rest is created during the cross-linking procedure and the structure consists of following partial connections: [1]

- Rubber
  - At first only physical, non-covalent bonds hold the material in piece, when cured a number of sulphuric bridges give the rubber its specific properties.
- Rubber-metal interface
  - During post vulcanization connection all links are formed by free chains which eventually settle in metal surface over time.
  - While curing the polymer macromolecules are heated, very mobile and tend to fill the dents more often.
- Metal subsurface layer
  - Material integrity in nonmetal layer depends on treating methods, still only chemical bonds are present. Cohesive force is influenced by depositions chemical character and thickness.

3.5 Gluing

Physical and chemical links develop on the entire contact area of glued materials right after applying adhesive. Influence of the mechanical links take part in the overall strength, especially for the usual low viscosity adhesives fill the cavity more easily (according to surface

energy as well), but in this case a covalent bond creates the most of adhesion force. Modification of the areas connected is usually identical to surface treatment when cured bonds are created. [1, 10]

Glued connections confirm their vast variety of use and begin to dislodge or improve conventional mechanical linkage on everyday basis worldwide.

3.5.1 Structure of glued bond

Best way to connect steel with already vulcanized rubber. The glue forms new interface consisted of mechanical and chemical joints on both sides as indicated below (Fig. 11). As the glue reacts and forms macromolecules a number of entanglements is formed on the interface giving the opportunity to create more mechanical and non-covalent bonds. Post vulcanization bonding enhances opportunities in creation of various components. Gluing is largely dependent on good wetting. In order to create firm connection a very obtuse wetting angle is demanded. Thus the adhesive fills all surface vacancies ensuring good linkage. [2, 20]

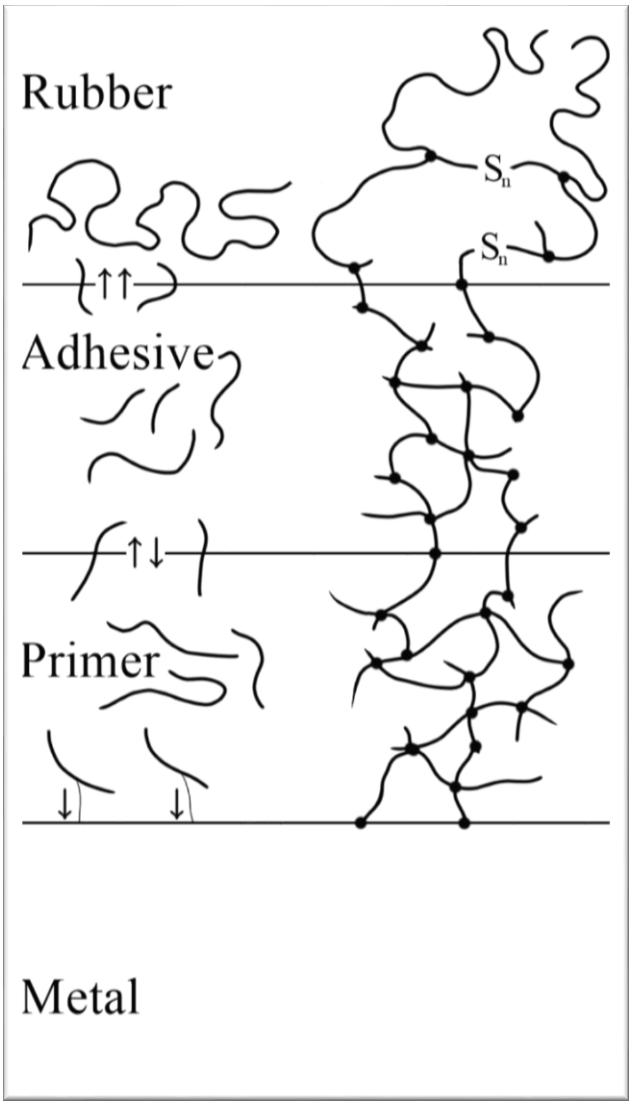

Figure 11 – Approximate structure of glued bond

The bond between the two materials is created during the crosslinking procedure and the structure consists of following partial connections: [1, 2, 12]

- Rubber
  - Often a vulcanized component is treated. Surface preparation may consist not only from regular degreasing but also from surface "activation" when a flame or plasmatic corona disrupts tail groups causing oxidation.
- Rubber-adhesive interface
  - Application of the adhesive, mostly in solution form connective layer, filling the cavities in rubber surface thus creating stronger adhesion.

  - Crosslinking process at high temperature guarantees new form of covalent bonding between rubber and adhesive. This of course is significantly dependent on the chemical nature of the adhesive layer.
- Adhesive-primer interface
  - Principal is similar to rubber-adhesive interface, only large number of crosslinks are created between the layers.
  - This of course is ensured via ideal material compatibility. Diffusion process and external crosslinking is a subject of interest while using primer-adhesive setup.
- Primer-steel interface
  - Primer deposit, like the adhesive works through solvent, enhancing the wetting capabilities. Chemisorption during the crosslinking process ensures covalent bonding with the metal surface.
  - Primer often serves as preservative to prevent unwanted intrusion of the freshly treated surface. Useful during storage.

3.6 Vulcanization

The curing process develops a strong connection, created between the surface layers of non-vulcanized rubber and metal parts. While curing a non-covalent in combination with covalent forces connect metal and rubber which are considered the strongest bonds of all listed types. [1]

3.6.1 Structure of cured bond

The Figure 12 represents vulcanized structure, where the macromolecules, connected between themselves and the copper sulphide layer via sulfur crosslinks form a strong joint on the metal interface. This type of linkage is strong not only due its many mechanical entanglements and electrostatic forces but also thanks to strong covalent bonds which were proved on brass surface. The C = C double bond in polyisoprene works as an active place to all covalent bonding. Copper contained in brass easily creates copper sulfide with sulfur from rubber compound. Therefore a function sulfur crosslink is created between rubber and metal for the benefit of connection durability. [2, 21]

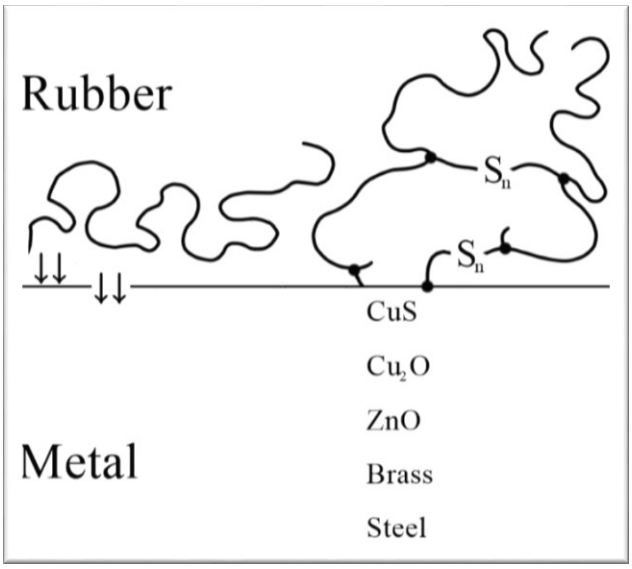

Figure 12 – Vulcanized bond structure

The bond between the two materials is created during the crosslinking procedure and the structure consists of following partial connections: [1]

- Rubber
  - Number of mechanical links develop in vulcanization process, mostly however the covalent bond between Sulphur and copper sulphide connects the material in chemical way.
- Copper sulphide layer
  - As listed in the above, covalent bonds between CuS and Sulphur are responsible for the chemical adhesion.
- Brass
  - Metal surface usually consists of the steel core, covered brass which is considered excellent at preventing corrosion. Brass layer contains ZnO in its structure, mostly then on the surface, followed by Cu_2O, followed by CuS. Cohesive force is influenced by the character of the compounds and layer thickness.

The strength of system is equal to strength of the weakest part and since the vulcanized connection is solid, most fractures occurs within the rubber structure. [1]

4 OTHER BENEFITIAL TESTS

4.1 Fillers examination

Payne in referred that the effect is found in different between zero and infinite storage modulus (zero and infinite strain in practice), but since this is technically impossible a very low and high strain is applied. [22]

When the polymer matrix is filled with attractive nanoparticles, mechanical behavior can be described in the framework of superposition approach. Total stress tensor (τ) in this approach is represented by a sum of two stresses:

$$\tau = X \cdot \sigma_m + \sigma_f^{net} \tag{1}$$

Where σ_m is the viscoelastic stress in the matrix due to stretching and orientation of polymer chains, σ_f^{net} represents attractive interactions between the particles and X imply hydrodynamic reinforcement of the polymer matrix. With spherical particles with hard surface such as carbon black and silica, X can be calculated in definitive way [23]:

$$X = 1 + 2{,}5 \cdot \varphi + 6{,}2 \cdot \varphi^2 \tag{2}$$

Where φ stands for the volume fraction of the filler particles. Equation furthermore reduces to $X = 1 + 2{,}5\varphi$, which is the Einstein's formula in the limit of small load. In the case of highly elongated particles, X is given as: [22]

$$X = 1 + 2 \cdot \varphi \cdot \left(1 + \frac{A}{15}\right) \tag{3}$$

Where A figures the stress-shape coefficient:

$$A = \left(\frac{r^2}{2 \ln r}\right) \tag{4}$$

For r is the aspect ratio $r = l/d$ (l is the particle length and d its diameter). Equation (3) can be also used in the case of semi-flexible particles such as carbon nanotubes, only one should take the persistence length instead of the particle length for estimation of the aspect ratio. Thus, we consider only hydrodynamic interactions between filler particles and the polymer matrix and neglect possible attractive interactions between them. [24]

In essence a stress on strain sweep in form of storage modulus in filled rubber compound is measured. This became popular with increase in usage of silica. Experiment runs on moving die rheometer and test can be performed on both cured and uncured samples. Current testing solutions often offer combination of vulcanization characteristics test and Payne effect on single specimen as the mechanical principle remains the same. Test settings depends on the curing state of the sample, so it runs at various temperatures, but effect detection at 60 or 100 °C is the most frequent. Continuously applied strain illustrates amplitude of the sinusoid and typically starting at 1 % and going up to 100 %. ASTM 6201, 6204 and 6601 are related standards. [25]

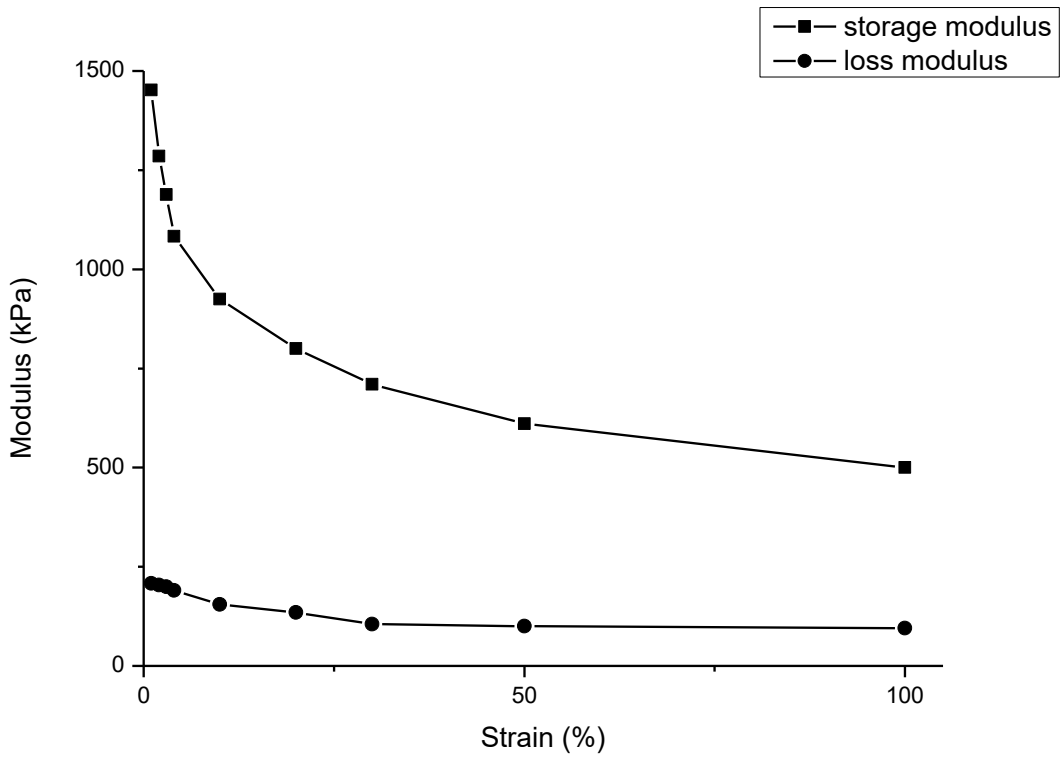

Figure 13 – Typical example of the Payne effect test result

Large drop in storage modulus (G´) from is typical from 1 – 20 %, after 20 % modulus levels and at infinite strain a plateau should be observed. Delta G´ deferential is the definitive result of the entire test method. During the process a weakening of the filler network – disruption of Van der Waals forces in CB or Silica occur. Result is commonly evaluated even pass or fail. Better the bonding, the lower the drop in storage modulus. In thread tire compounds, delta G´ drop around 350, 400 kPa is considered an excellent result. So basically this test describes a filler to filler interaction. [25]

A certain similarities were established in different matrix systems (elastomer and thermoplastic). Mainly due to storage modulus recovery of the filler structure. [24]

4.2 Basic abrasion test

Abbreviation xWAT stands for wheel abrasion test, where x marks the tested material, like steel, rubber or just selected coatings. Method gives repeatable results especially for studies of material wear and friction under wear if the correct method is applied which depends on studied material and test settings such as dry or wet surroundings, torque, exposure time, rpm, abrasive material etc. Typical outcome in graphic form shows wear, friction or energy loss dependency on selected variable.

Figure 14 below describes that input torque *T* is a product of the applied load *N*, wheel radius *r*, it is possible to determine friction [26]

$$T = \mu N \cdot r \tag{5}$$

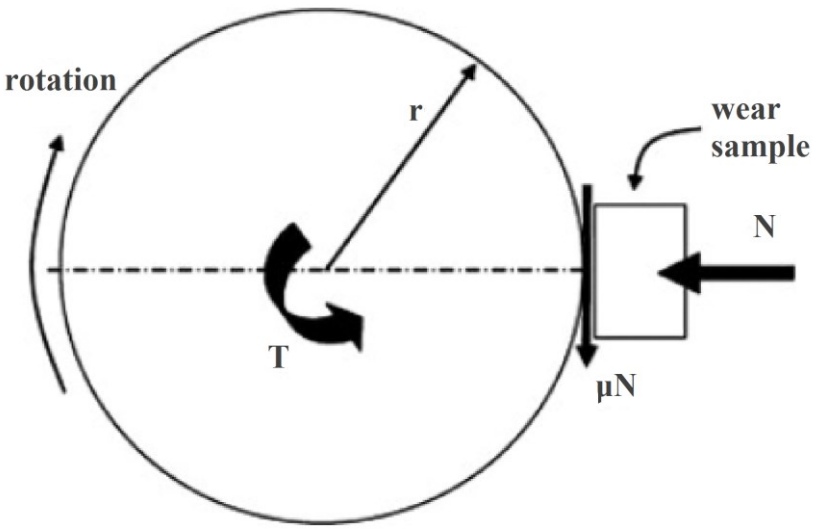

Figure 14 – Forces on the abrasion wheel [26]

II. ANALYSIS

5 SAMPLE PREPARATION

5.1 Compoundation

In order to prepare test specimen a rubber compound was created using internal mixer at 6,5 rps to mix rubber and carbon black before continuing further on the double calender. After 8 minutes the compound was transferred to calender, where the other elements were added in order listed in table below. Entire mixing process took 19 minutes of machine time to complete. Gap between the cylinders was adjusted to 1,2 and 1,9 mm and the peripheral speed of cylinders set to 9,0 and 12,0 rpm.

Table 2 – Material composition

Component	PHR	Weight [g]	Time [min]
NR 3L	100,0	254,62	0 – 5
CB 339	50,0	125,78	
ZnO	3,0	7,55	5 – 11
Stearic acid	1,0	2,53	
Antioxidant	1,5	3,83	11 – 15
Activator	2,5	6,31	15 – 17
Sulphur	1,7	4,30	17 – 19
Total	158,7	404,92	19

Presented compound is suitable for further research mainly to its simple reproducibility. Formula is not remotely similar to tire tread rubber composition, so high durability and structural strength was presumed. Because of no need for greater elongation and moderate amount of reinforcing filler an absence of oil and other softeners is intentional.

5.2 Vulcanization characteristics

Using the rotary rheometer MDR3000 type plate-plate a clear characteristics was obtained as seen on exemplary (Fig. 15). The mass of at least 5 grams of compound was treated at 150 °C for just over 15 minutes to reach complete required outcome, excluding reversion.

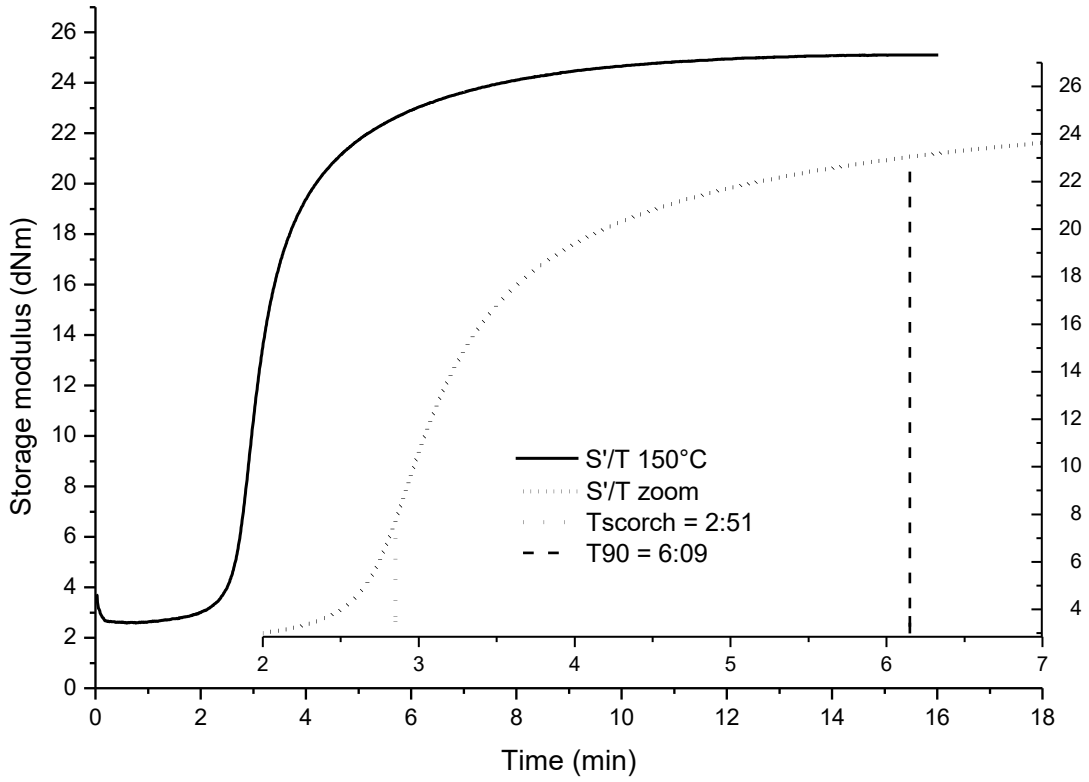

Figure 15 – MDR3000 result at 150 °C

Further on the test ran at 140, 150, 160 and 170 degrees Celsius to give basic information about thermal dependence of the compound while curing. Processing the rubber at 150 °C seems ideal for laboratory testing due to its relatively short T_{90}, set at 6 minutes and 9 seconds. Such time allows worker to quickly process great amount of cured rubber for ongoing testing with 150 seconds of reserve time to abort the process if needed. Processing safety with given amount of sulfur is ensured, but since the time border is crossed, curing runs at 0,31 dNm·sec^{-1} (peak rate) reaching T_{50} only after 1 minute, shown as a steep rise between T_{10} and T_{90} on the Figure 15.

Table 2 below represent detailed characteristics obtained from measurement at given temperatures. The most common rule tells that with every 10 °C increase of temperature the curing time needed reduce to half.

Table 3 – MDR3000 results

T [°C]	T_{scorch} [s]	T_{10} [s]	T_{50} [s]	T_{90} [s]	peak rate [dNm·s^{-1}]
140	301	322	382	686	0,19
150	171	186	221	369	0,31
160	91	101	121	194	0,51
170	57	63	76	112	0,82

5.3 Pressure molding

Hydraulic pressure molding machine was pre-heated to 150°C together with steel cover plates and square frame 125 mm of length and 2 mm thick. Assuming density of compound close to 1 g/cm^3, a mass of 31,25 plus 3,13 grams rubber was placed in the heated frame, covered with plates and placed to the pressure molding machine. System was cured for 6 minutes and 15 seconds at sealing force 250 kN.

Cured rubber plates of 2 mm estimated average thickness were used to cut a dumbbell and stripe specimen.

6 TESTING

All the examination described further on was executed on single series of rubber compound.

6.1 Quasistatic tests

6.1.1 Simple tensile test

Elastomer limits under quasistatic loading conditions

Method described in ISO 37. The measurement is performed on a tensile strength tester, calculating current strength and elongation. Test specimen commonly formed in the shape of a dumbbell less likely a paddle or eight. [27]

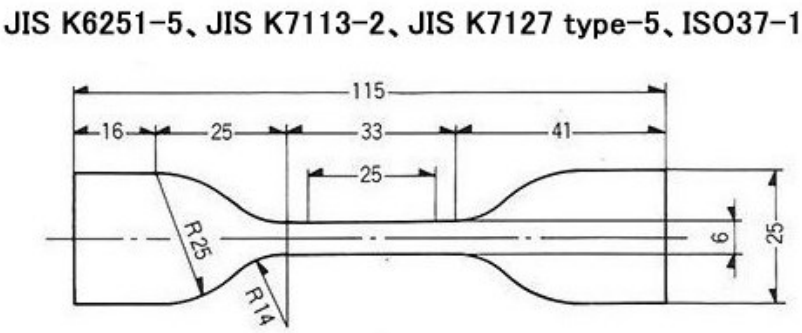

Figure 16 – Dumbbell test specimen, type 2

Stretched at constant speed the software evaluates the strength and adequate prolongation which results in tensile curve. From the 0,05 to 0,25 % of total data amount a Hooke's law is calculated using simple linear trend, which however applies directly to conventional materials only. [28]

$$\sigma = E \cdot \varepsilon \tag{6}$$

Where σ is stress, ε stands for relative prolongation and E represents material Young modulus. In order to define the dimension variation:

$$\varepsilon = \frac{L - L_0}{L_0} \tag{7}$$

Where L is the actual length and L_0 is the original length of the specimen.

Elastomers however show more complicated behavior under any loading conditions. Therefore a modulus at certain elongation serves as the agreed result. Complications may appear while measuring conditions are selected improperly. Rubber type materials require higher clamp movement speed, typically from 500 mm/min. Invalid test is considered in case of the specimen slip from either of clamps or rupture appears out of „work zone“. [27]

Description of tensile test for determination of overall compound toughness

The procedure was executed in terms of recommendations in ISO 37 on the Testometric M500 device which uses computer software allowing to run any user defined programs. Also contains heat chamber for temperature dependent observations. Every sample was elongated until failed. Average thickness of specimen was 2,5 mm.

For our test the loading conditions has been chosen as follow:

- 500 mm/min movement rate
- Type 2 dumbbell specimen

Figure 17 – Testometric M500

Results and discussion

Graphic results (Fig. 18) describe typical behavior of the rubber compounds with standard S curve with rather large deviation from the average, especially in the final settled M300 modulus. Given that maximum tensile force in average ranged in hundreds Newton, providing a reasonable. Please bear in note, that overall average results above do not show any actual data and the first 50 % of elongation is only figurative.

As seen in Table 3, the average breaking point was detected at (360 ± 40) % of elongation and (27,8 ± 1,2) MPa of load. Given that material easily withstands 10 MPa and 150 % elongation a boundary conditions for peel test, hysteresis and dynamic peel test are not critical as regards structural integrity of the material.

Choice of a correct compound is crucial for the resulting adhesion. Different types of rubber show different behavior, chemical and mechanical properties and specific tolerance to adhesives.

Table 4 – Tensile test numerical review

spec	σ_{max} [MPa]	ε_{max} [%]	M50 [MPa]	M100 [MPa]	M200 [MPa]	M300 [MPa]
1	26,55	335,15	2,59	5,54	14,56	23,82
2	28,23	411,15	2,12	4,36	11,95	20,40
3	26,81	371,90	2,17	4,48	12,38	21,15
4	28,93	406,25	2,21	4,37	11,68	20,54
5	26,69	303,05	3,21	6,66	15,77	26,47
6	29,64	325,60	3,04	6,41	15,67	26,90
AVG	27,81	360	2,56	5,30	13,67	23,21
SD	1,20	40	0,50	1,00	1,80	3,00

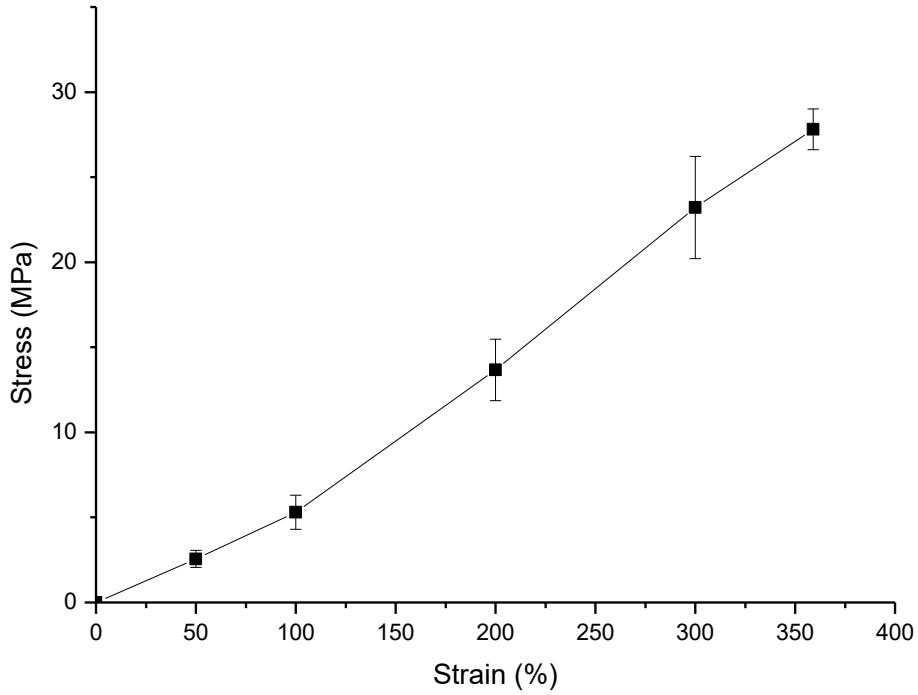

Figure 18 – Tensile test average curve

6.1.2 Shear test

Description of shear test for determination of the ideal setup

The main goal was to create a test specimen which will fracture one of the materials cohesive during test. This was performed using steel substrate and already vulcanized rubber bonded via methyl cyanoacrylate superglue. Both surfaces were treated with fine sandpaper and iso-propyl alcohol before the glue was applied. Samples were tempered in dryer at 50 °C for 30 minutes to even their thermal state.

At first a high quality glue (HQG) applied on rubber and steel separately held both layers very firmly, so that structural break in rubber occurred, see on Figures 19 and 20. Tempered rubber only defected connection on steel (Fig. 21). The multi-layer technique took place in next attempt (Fig. 22), sample was coated three times on each substrate after the previous deposit polymerized. On the fourth application the materials were connected.

Results and discussion

Overall sample preparation took roughly 60 minutes from start to handling strength, then another day to ensure the polymerization of the cyanoacrylate glue was complete.

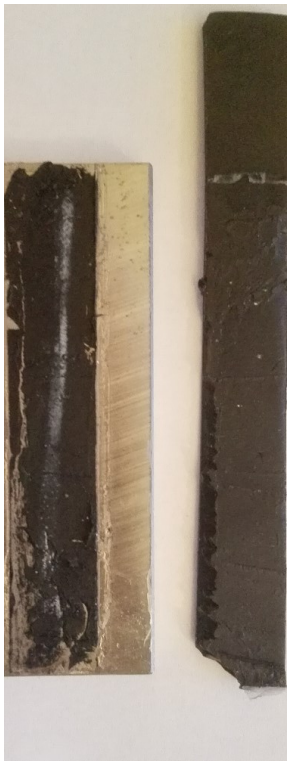

Figure 19 – Cohesive fracture of rubber (treated, tempered both, HQG)

Figure 20 – Combined fracture (treated, tempered rubber, HQG)

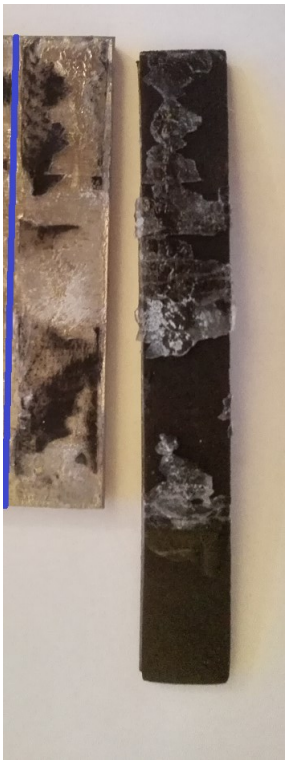

Figure 21 – Combined fracture (treated, tempered both, LQG)

Figure 22 – Cohesive fracture of glue (treated, tempered both, LQG)

Figure 19 shows most promising results. For the further testing a HGQ was used exclusively, treating and tempering both layers at given conditions. Structural failure in rubber is believed to be the most common and the most wanted example in any common mass production. Sample preparation, process conditions as well as glue quality confirm significant impact on the final outcome.

6.1.3 Peel test

Adhesive force under quasistatic loading conditions

Peel test (Fig. 23) is defined by ISO 813. This probably the simplest, most effective and widely used method of testing connections. Rubber specimen of defined dimensions is fixed to a metal strip at most of its area, where the loose end is clamped to tensile strength tester which moves the clamp at typical 50 mm/min. To increase overall efficiency a notch on the materials interface is created before start. This reduces probability of crack initiation in the loose end of the rubber. [29]

The advantage is that the rate of delamination and the focus of failure can be controlled precisely. This stems from a very high stress concentration that exists at the point where the coating lifts off the substrate. [30]

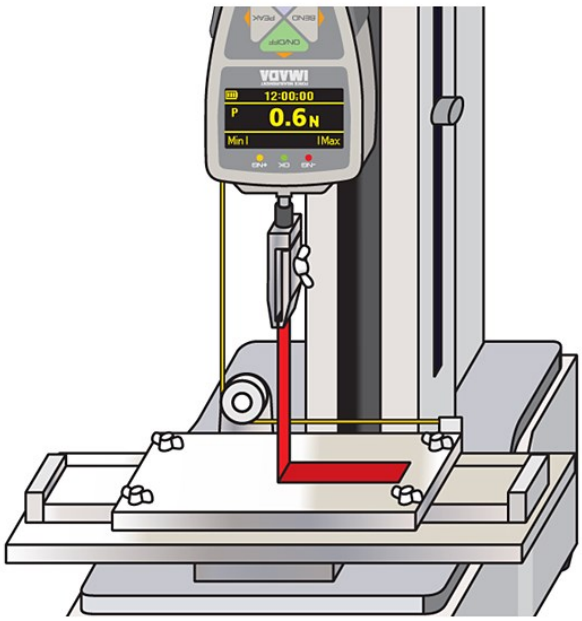

Figure 23 – Peel test setup [29]

There are several standard procedures (BS 903, ISO 813 and ASTM D429) in more varieties. General differences lies in dimensions of the samples, however the principle remains the same.

Let R be a cohesion, represented as:

$$R = \frac{F}{b} \cdot (\lambda - \cos\varphi) - W \cdot t_0 \tag{8}$$

Where F is loading force, b is width, λ is prolongation, φ is peeling angle, W is strain energy density and t_0 is thickness of the rubber sample in an unloaded condition.

Assuming that the peeled material is not deformed, $\lambda = 1$ and the relation transfers to the following form:

$$R = \frac{F}{b} \cdot (1 - \cos\varphi) \tag{9}$$

Cohesion in case of $\varphi = 90°$:

$$R = \frac{F}{b} \tag{10}$$

If $\varphi = 180°$, equation turns in the form:

$$R = 2 \cdot \frac{F}{b} \tag{11}$$

The 180° method corrects potential inaccuracies incurred during 90° peel test. [29]

Deviations from linear elastic behavior become more significant at low peel angles so that the peeling operation approaches the shear failure of a lap joint. At large peel angles such high levels of pre-load can significantly reduce the peeling force. [31]

Description of peel test for determination of bond strength

Basically any tensile device with appropriate assemble may serve for the peel test purposes. In this case a tear and fatigue analyzer investigating the fatigue crack growth of rubber materials independent on test specimen's geometry is shown in the Figure 28 (see 6.2.2). For the wide range of applications TFA is suits needs of any peel test.

Test specimen, prepared as seen most suitable in previous evaluation (6.1.2 Shear test) were used to cover needs in peel test. Average width test specimen was 10 mm.

For our test the loading conditions has been chosen as follow:

- Up mounted, 10 mm/min movement rate at 90°
- Up mounted, 10 mm/min movement rate at 77,5°
- Bottom mounted, 10 mm/min movement rate at 90°
- Bottom mounted, 10 mm/min movement rate at 77,5°
- Bottom mounted, 80 mm/min movement rate at 90°

Results and discussion

Every peak (Fig. 24) represent the force needed to cause fracture. Standard evaluation method is focused on the average value of the positive peaks. Table below submit standard results, which are overall not suitable for any application. Considering only maximum force developed the peel test 53 N in average, values drops down one system compared to tensile result peaking 741 N at max. With regard to the requirements listed above (see 3.3), bond strength is not equal nor higher than the strength of rubber therefore a very weak example was examined. To ensure certain quality at least hundreds Newton must have peaked. For the methodology any loading conditions seem suitable given to fairly similar standard deviation, although mounting assembly to upper receiver may influence the method greatly listing much lower values and thus more effective disruption of the bond.

Table 5 – Peel test numerical review

Mount position	Bottom			Upper	
Peel angle/ rate	90/ 10	77,5/ 10	90/ 80	90/ 10	77,5/ 10
AVG [N/mm]	3,7	5,0	5,3	1,8	2,0
SD [N/mm]	0,7	0,7	1,0	0,5	1,1

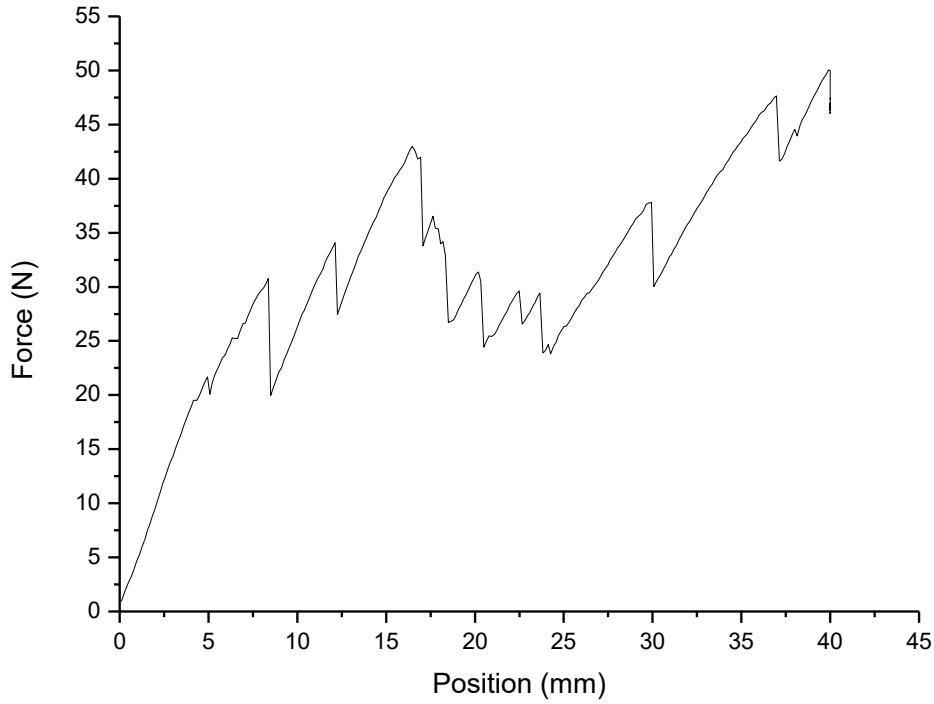

Figure 24 – Peel test result UP_90/10

6.2 Dynamic test

6.2.1 Hysteresis

Rubber softening under dynamic loading conditions

Over forty years since Mullins published review on the phenomenon still no general agreement has been found either on the physical source or on the mechanical modelling of the effect. [32] Up to this date a number of papers were published on the Mullins effect and constitutive models vary from author to author.

In order to account for the elastomer softening, Simo created one of the first models, based on a phenomenological definition of the strain energy. [33] Designed to fit the hyperelastic stress–strain responses of rubber-like materials submitted to the deformation gradient F by a reducing parameter of the Kachanov type [34]:

$$W(F) = (1 - d) \cdot W_0(F) \tag{12}$$

The $W(F)$ is the strain energy, $W_0(F)$ the resting strain energy, $(1 - d)$ defines a reduction factor, which may cover any physical phenomenon like chain cracks, microvoid formation, microstructural damage etc.

There are several hyperelastic material models that are commonly used to describe rubber another elastomeric materials based on strain energy potential or strain energy density. The hyperelastic models for rubber material can be expressed in the following general form:

$$W = W_I(\bar{I}) + W_I(J_{el}) \tag{13}$$

Where W_I (I) is the deviatory part of the strain energy density of the primary material response; W_J (J_{el}) is the volumetric part of the strain energy density. I can be expanded further to I_1 and I_2, which are an alternative set of the invariants.

One of the most common constitutive model without Mullins effects can be expressed by polynomial series:

$$W = \sum_{i+j=1}^{N} C_{ij}\,(\bar{I}_1 - 3)^i(\bar{I}_2 - 3)^j + \sum_{i+j=1}^{N} \frac{1}{D_i}(J_{el} - 1)^{2i} \tag{14}$$

Where C_{ij} and D_i are material constants for a given rubber compound, I_1 and I_2 are alternative set of the invariants. When C_{10}, C_{01}, and D_1 coefficients differ from zero, equation can by simplified to the Mooney-Rivlin model:

$$W = C_{10}(\bar{I}_1 - 3) + C_{01}(\bar{I}_1 - 3)(\bar{I}_2 - 3)^j + \frac{1}{D_i}(J_{el} - 1)^2 \tag{15}$$

Luo and Mortel published validation that the purposed approach predicts results very close to measured experimental values. It is indicated that the first loading-unloading cycle removes the Mullins effect by approximately 80 % on this typical case. [35]

On the anisotropy of mechanical properties, Sharadin et al describes how material softens along the extension axis. Also this softening does not, influence the structural rearrangement along the orthogonal prolongation axis and differ the mechanical properties of the material lengthways the transverse axis in any way. If the elastomer with carbon nanofibers is loaded along one of its axis, the structural rearrangement and variation in mechanical properties occur in all directions. [36]

Description of hysteresis for determination of dynamic crack growth analysis

Method for testing energy loss in material, or rubber softening as often described. Set was performed on the Testometric M500 device illustrated earlier (see Fig. 17). The conditions set to clamp reach desired elongation, then back to zero strain. The specimen of rectangular shape was elected, 10 mm width and 30 mm of work length. Average thickness is 2,5 mm. Although that loading and unloading curve both can be described fairly simple by third degree polynomial equation, the easiest and most precise way to evaluate data was the "integrate" feature of the OriginLab software.

For our test the loading conditions has been chosen as follow:

- 50 mm/min movement rate
- 20, 40, 60, 80 and 100 % elongation
- 5 repeats on each step

Results and discussion

See the illustration (Fig. 25) of the greatest difference in between every step at its maximal and minimal energy loss. The dotted lines represent first strain to any given maximum where the solid line shows minimal dissipation at the last step at current elongation.

Table 6 – Energy loss due to rubber softening

rep.	W_{20}	W_{40}	W_{60}	W_{80}	W_{100}
0	4,18	7,94	12,75	19,30	26,94
1	1,05	5,33	9,32	14,40	20,28
2	0,76	5,33	8,68	14,02	19,64
3	0,54	4,82	8,33	13,05	18,77
4	0,29	4,75	8,10	13,00	18,55

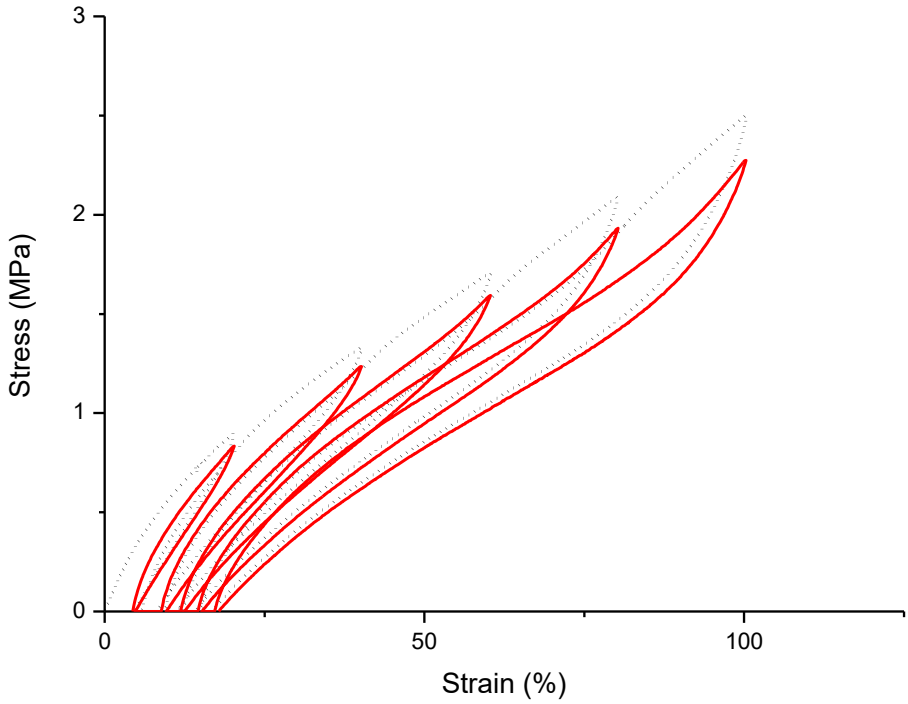

Figure 25 – Rubber softening

6.2.2 Fatigue peel test

Tearing energy under cyclic dynamic loading conditions

An important quantity for fracture mechanical investigation is the tearing energy, T i.e. the energy released per unit area of crack surface growth. Rivlin & Thomas formulated the tearing energy for elastomers. It proposes that the strain energy release rate is the controlling parameter for crack growth and it is mathematically defined as [37],

$$T = -\frac{\delta W}{\delta A} \tag{16}$$

Where, T is tearing energy, W is the elastic strain energy and A is the interfacial area of crack and partial derivative denotes that no external work is done on the system.

As already mentioned previously, there are many factors that affect the fatigue process in rubber and many approaches to analyze fatigue behavior. Experimental analysis based on mechanical loading are most common. By definition, mechanical fatigue involves crack nucleation and growth due to fluctuating loads (Fig. 26). The driving force of load can be

represented by any of various parameters associated with specific analysis approaches: strain, stress, strain energy density, energy release rate, etc. The value of mechanical loading is usually determined as maximum, alternating, minimum and mean loading, and/or the R-ratio [37].

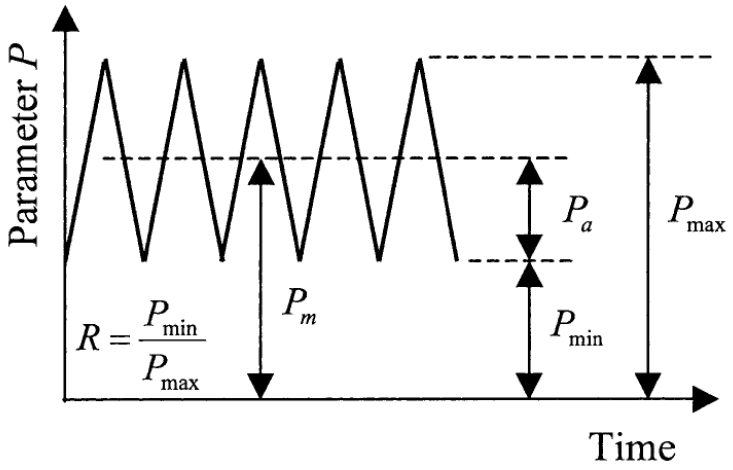

Figure 26 – Schematic visualization of cyclic dynamic loading

Widely used rubber fatigue test at tensile or combination of tensile/compression mode by using of standard test specimens (ASTM D4712 Type C, dumbbell specimen) monitors the behaviour of the material under alternating load. From results of this test, the difference between a quasistatic load and a fluctuating load is visible. Quasistatic load does not cause fatigue failure, even at high, sub-fracture levels. In contrast, fluctuating load can cause fatigue failure, even at low levels. Although quasistatic loads do not cause fatigue failures even at high levels it can cause failures due to steady, time-dependent crack growth in the case of elastomers that do not exhibit strain crystallization, or in the presence of environmental attack. [38]

The cyclic dynamic loading conditions are the reason for the stiffness loss in rubber materials, whereas this phenomenon has been treated extensively. The rubber material is subjected to a rapid decrease in stiffness due to applied first few loading cycles, which was demonstrated by Mullins [38, 39]. Under next proceeding of cyclic loading beyond the first few cycles, stiffness loss is known to follow a semi-logarithmic trend [40]. The rate of this trend is smaller than the initial Mullins effect, at least until the crack nucleation/initiation life is approached. Because the acceleration of the initiated crack due to the cyclic loading of the rubber specimen, the initiated crack accelerates. Thus the rate of stiffness loss increases until the loading is finished or until the test specimens is totally ruptured [41].

Gent, Lindley and Thomas determined experimentally the fatigue crack growth (FCG) rate *da/dn* in dependence on the crack driving force or tearing energy, *T* respectively for rubber materials. [42]

Figure 27 shows the typical relationship for a rubber material in a double logarithmic plot. Lake and Lindley divided this plot into 4 regions that characterize different tear behaviors. The FCG rate *da/dn* depends on the tearing energy *T* in each of the 4 regions in a characteristic manner. [43]

As long as the value of tearing energy *T* is lower than T_0, FCG proceeds at a constant rate *r* and the FCG is independent of the dynamical loading, but affected by the environmental attack.

$$T \leq T_0 => -\frac{da}{dn} = r \tag{17}$$

In region II between T_0 and T_1 one finds a transition between a nucleation and propagation of crack:

$$T_0 \leq T \leq T_1 => -\frac{da}{dn} = A \cdot (T - T_0) + r \tag{18}$$

After this transient state the crack propagates in a region between T_1 and T_C of stable crack growth which is denoted as region III. The relationship between FCG rate *da/dn* and tearing energy is described by Paris and Erdogan [44] with the power-law:

$$T_1 \leq T < T_c => -\frac{da}{dn} = b \cdot \Delta T^m \tag{19}$$

Where *b* and *m* are material constants.

In the last region, IV, the tearing energy T_C proceeds to the instable state of FCG and the FCG rate will become essentially infinite.

$$T \approx T_c => \frac{da}{dn} = \infty \tag{20}$$

Region III was utilized as the region that corresponds most closely to FCG rates found in the engineering fatigue range. In the industrial usage analyses of SENT and PS specimens mostly are performed according to this region to compare the stable crack growth and thus to compare the behavior of crack propagation with respect to rubber composition.

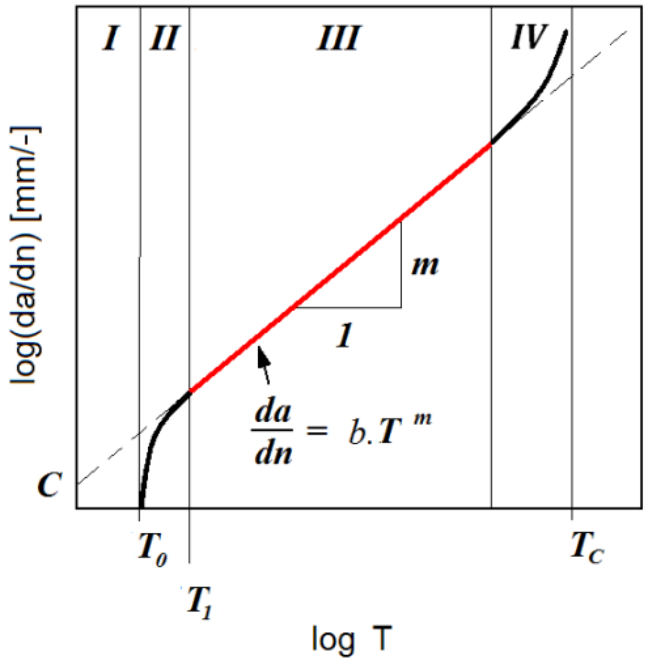

Figure 27 – Double logarithmic plot of FCG rate, da/dn vs. tearing energy, T for rubber material [43]

Description of TFA for determination of dynamic crack growth analysis

It is possible to measure up to 9 test specimens simultaneously. Because of implementation of 3 independent engines, three different loading conditions are possible to be applied. It is possible to apply the analysis of different loading modes (sine-, triangle-, pulse loading, free loading curve), within the frequency range 0,1 – 50 Hz. Each upper clamp attachment of test specimens is fixed to the load cell and its corresponding test specimen clamp attachment is connected to a separate computer-controlled stepping motor to ensure constant pre-stress during the whole time of testing. The crack growth of each rubber test specimen is monitored through an image process system with high-speed CCD camera mounted on the linear motion axis system. The camera moves along the xy-axis from test specimen to test specimen and takes a picture of the concerning test specimen. The picture is then transferred to a frame grabber and stored. After the picture has been digitalized the software localizes in situ the crack position and determines the contour length by following the black and white boundary line of the crack. The detailed description can be found e.g. in Eisele et al [45].

Figure 28 – Photo of Tear and Fatigue Analyzer – the version of 3 electro drives

For our test the loading conditions has been chosen as follow:

- Loading frequency 5 Hz
- Waveform: sinus
- Loading amplitude: vary in dependence on tearing energy applied

Assembly is designed specifically for the TFA, taking place on one engine it's design allow the specimen to be inclined from 0 to 180 degree angle (*φ)* covering all possibilities. Free end of the rubber stripe is settled in the moving clamp while steel substrate firmly holds on the linear guide which by defined movement rate, coordinated with test setup ensures the observed area to remain in the view angle of the camera.

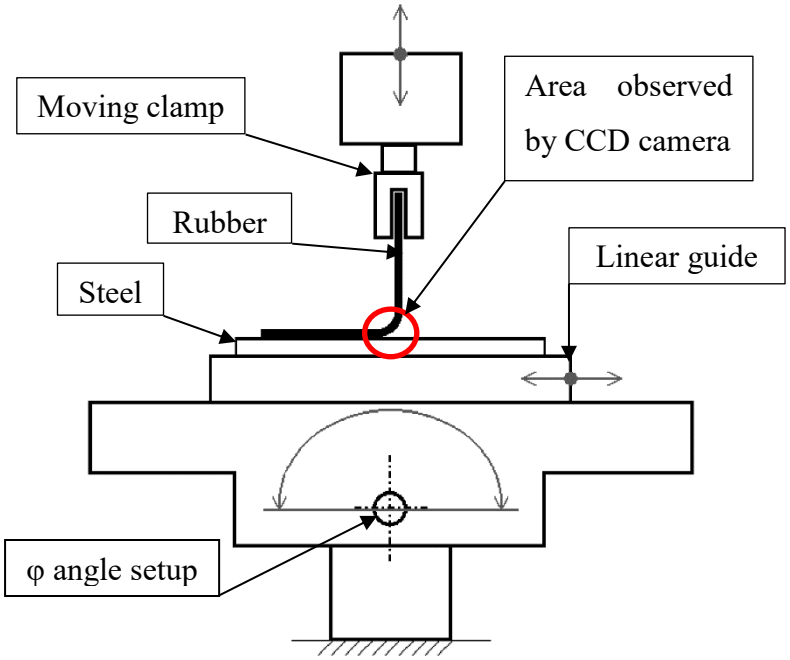

Figure 29 – Assembly's description

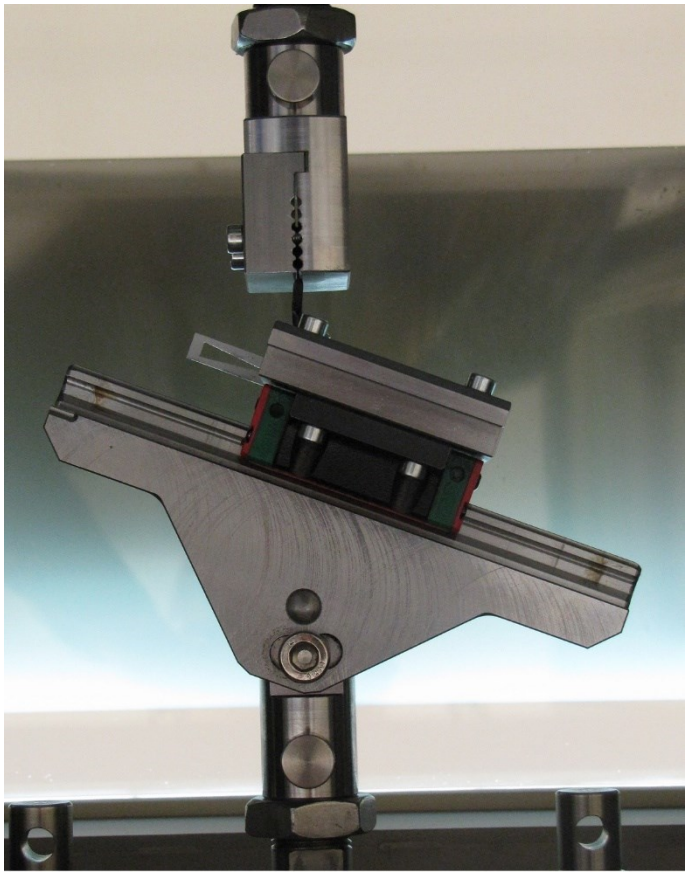

Figure 30 – Assembly in process

Results and discussion

The result of fatigue crack growth between the rubber and metal part is shown in the Figure 31. It is very clearly visible that with the increasing of tearing energy the fatigue crack growth rate increases as well. At the lowest tearing energy used T = 120 J/m^2 the fatigue crack growth about 1,00e^{-5} mm/cycles has been observed, however at the highest tearing energy, T = 850 J/m^2 the fatigue crack growth about 5,00e^{-3} mm/cycles has been determined. The fatigue crack growth rate values demonstrate the resistance of the bounding against tearing respective delamination both of the components.

It is very clear, from the data observed, that the bonding is of a very poor quality because of the fatigue crack growth rate in pure rubber matrix approximately is 10 times lower. [46]

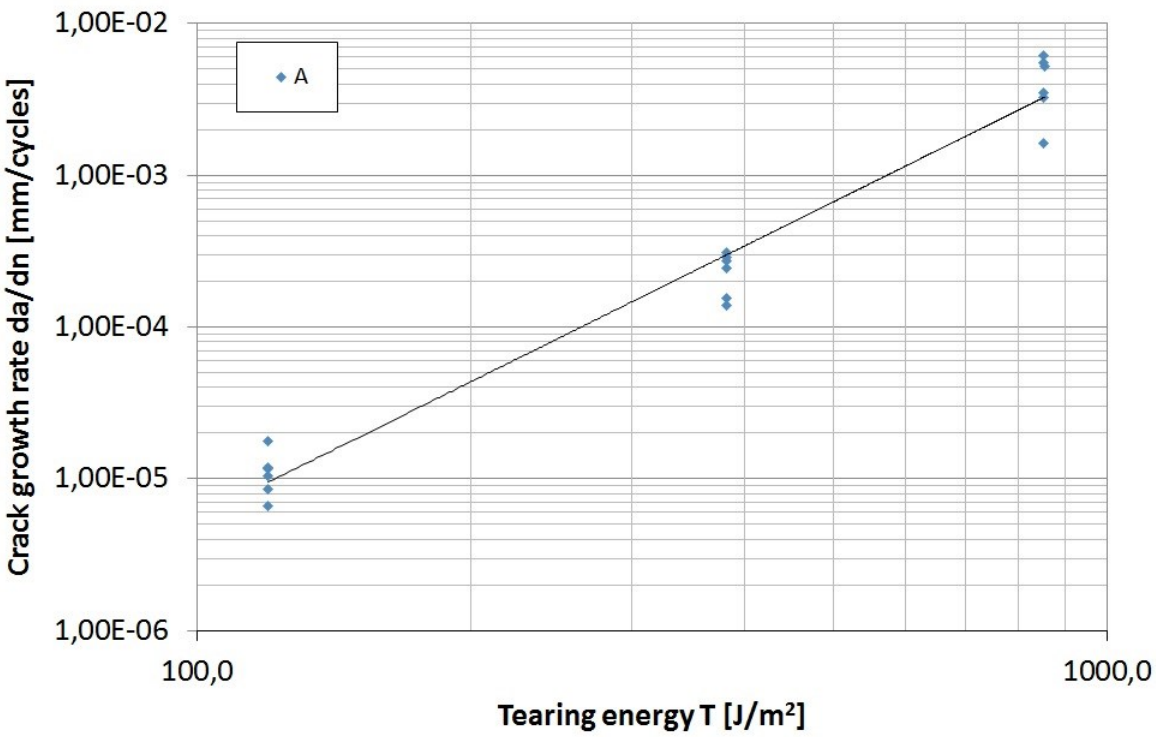

Figure 31 – FCG curves for rubber metal part.

6.3 FEM analysis

To complete the entering a deeply crude finite element models are presented (Fig. 32, 33), using Catia V5 software. For better understanding the problematics of rubber-metal part under load a FEM model represents approximate force distribution via triangular system on which a calculation is proceeded. Initial conditions, taken from peel test (see 6.1.3) were

implemented on the created model of the 90° setup with modifications, due to absence of greater skill in modeling overall. The rubber component is illustrated as a block with spherical curvature of 90°. The large block on the bottom is meant to be the steel substrate. Adhesive is figured by the small block between the two and because of the lack of materials, an epoxy resin was selected.

The initial load of 5 N, illustrated on Figure 32 serve for better understanding partition of the force applied, shown as a yellow cursors. Under such conditions only a small force is dispersed towards the adhesive, therefore a Mullins effect (see 6.2.1) is considered.

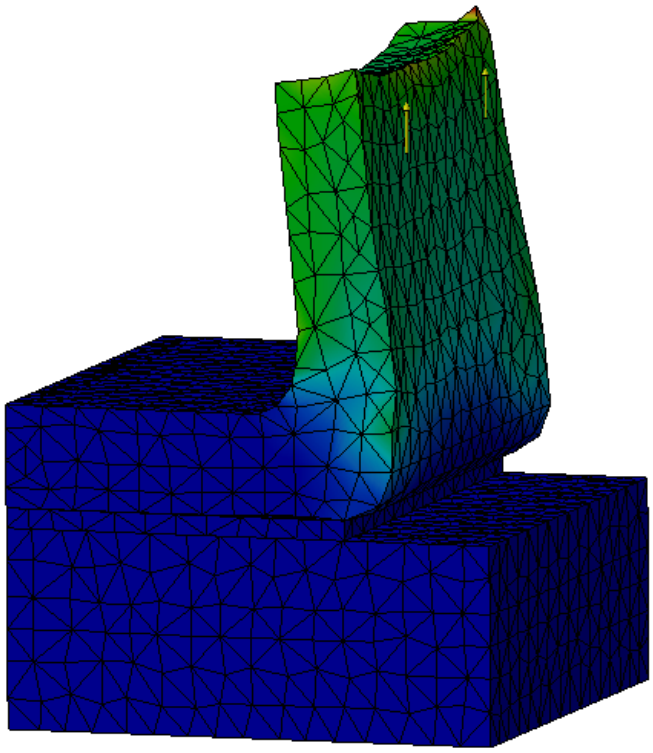

Figure 32 – Approximate FEM model of the first cycle deformation

The Figure 33 presents an example of actual bond failure with regards to the adhesive force, taken from peel test measurement. To simplify the evaluation a firm bond was settled on the steel-adhesive interface and the surface force density was set to 50 N/m^2. However the bond, evaluated as very weak before shown no tendency to transmit any of part the load applied and failed completely instead. This may be caused due to not quite accurate model, less likely to the anchorage of the single areas. At real conditions the rubber part is pulled straight upwards instead of deformed as shown. Nevertheless the crack is sure to develop on the rubber-adhesive interface.

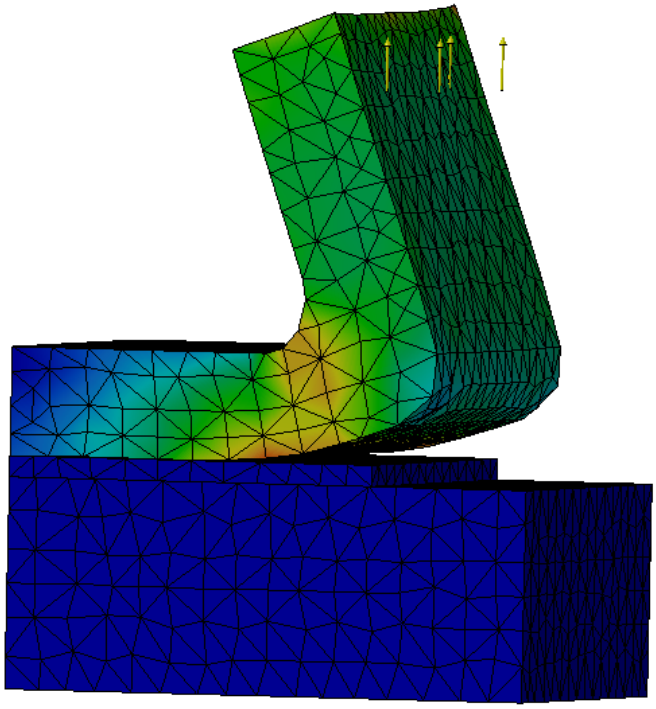

Figure 33 – Approximate FEM model of the created bond

CONCLUSION

The theoretical background should outline sufficient initial information for anyone at task of creating any listed bond type. Methods of surface preparation belong to the most common and most used given to simplicity or rentability of each single process and therefore are suitable for any production. Agents follow the agenda creating insight into the issue of adhesion choice as far as the rubber-metal bonding is concerned. While the materials are connected to each other a chemical phenomenon on the interface is described. At any form of created joint, a principle of the interface structure at any case is discussed regarding the manner the materials are put together. In order to involve the final stage of bond's life a number of testing methods are included. Put aside, the filler observation and surface wear is considered not suitable for the actual execution yet still important enough to take notice in further research therefore a little insight into the issue was provided.

As discussed on 6.1.1 importance of the rubber compound composition is yet subject of a following research. Tensile test determine how the elastomer behave under critical load and generates startup mechanical properties needed for further advance. Advantageous mainly due to fairly low cost equipment compared to fatigue peel test.

Even though shear test had been performed by hand, approaches current methods, based on optical review of the rubber-metal bond after tear analyze mostly. Fast and rather informative result is indeed suitable for production control, nevertheless data absence carry no scientific value and therefore no use for any possible research activities. Effective combination of fast execution and informative

Peel adhesion contains data with moderate informative value. Still quasistatic test but useful while the rough grip is evaluated. The graphic outcome as descriptive as it is still lacks other than minimum and maximum adhesion force. Setting of the peel angle and its impact on adhesion, especially in combination with other materials may provide rather interesting topic for possible successors.

Review on the Mullins effect shown considerable energy loss in initial loading cycles, therefore possible distort of results of the fatigue peel test. The softening decreases over time, but if relaxation does not occur, the results are not furthermore affected. In order to improve methodology it is preferable to neglect the initial data. Thus an actual course of action

has been established for the TFA results are most likely to determine exact fatigue crack growth rate, the amount of energy needed to initiate and spread the fracture also captured in time. The method has been validated and can fully be used for characterization of rubber-metal bonding behavior with respect to real loading conditions of rubber product.FEM has shown an insight at the rubber softening as well as the created bond failure. Method proved to be extremely useful and any analysis, using FEM models remain the subject of future interest.

As said before, given to TFA analyzer cost it is possible to determine approximate bond quality on a budget using highly equipped tensile tester. But for the definitive results, more closely related to reality of processes related to (not only) rubber fatigue a high end equipment, capable of simulating various load conditions will always provide better outcome.

BIBLIOGRAPHY

[1] ŠŮLA, Miroslav. *Pojení pryže s kovem.* Zlín: ČSPCH. 2007. 63 s. ISBN 978-80-02-01934-3

[2] CROWTHER, Bryan.: *The Handbook of Rubber Bonding.* Rapra technology LTD. United Kingdom, 2001. 3-97 s. ISDN 1-85957-394-0.

[3] Degreasing - Blast. *Surface preparation* [online]. Houston, c2017 [cit. 2017-05-01]. Dostupné z: http://www.surfacepreparation.com/applications/degreasing-blast

[4] KRAUS. V., *Povrchy a jejich úpravy* [online]. [8.7.2016] [cit 04-11-2016]. Dostupné z WWW: http://tzs.kmm.zcu.cz/POUcelk.pdf

[5] Uses Of Abrasive Blasting. *Is San Francisco - Shaking?* [online]. SanFrancisco, c2017 [cit. 2017-05-01]. Dostupné z: http://www.issanfranciscoshaking.com/marketing-and-advertising/uses-of-abrasive-blasting/

[6] WAKE, William Charles. *Adhesion and the formulation of adhesives*. 2nd ed. New York: Applied Science Publishers, 1982. ISBN 0853341346.

[7] BUDINSKI, Kenneth G. *Surface engineering for wear resistance*. Englewood Cliffs, N.J.: Prentice Hall, c1988. ISBN 0138779376.

[8] H. Leidheiser, Presented at the ACS, Division of Polymeric Materials: Science and Engineering, Fall 1986, Paper No.12

[9] Pre Treatment. *JMC Powdercoating* [online]. Melbourne, c2017 [cit. 2017-04-28]. Dostupné z: http://www.jmcpowdercoating.com.au/wp-content/uploads/2014/04/JMC-Power-coatng-PRE-PROCESS4.jpg

[10] KOLESKE, J. V. *Paint and coating testing manual: fifteenth edition of the Gardner-Sward handbook*. West Conshohocken, PA: ASTM International, 2012. ISBN 0803170173.

[11] Galvanization process. *Corbec* [online]. Lachine, c2017 [cit. 2017-05-1]. Dostupné z: http://www.corbec.net/eg/galvanizing.php

[12] COGNARD, Philippe. *Handbook of adhesives and sealants*. Boston, Mass.: Elsevier, 2006. ISBN 0080447082.

[14] MALÁČ, Jiří. *Gumárenská technologie: 2 kaučuky*. Zlín, 2012. Dostupné také z: http://www.utb.cz/file/36219

[15] Bisphenol A diglycidyl ether. In: *Wikipedia: the free encyclopedia* [online]. San Francisco (CA): Wikimedia Foundation, 2001- [cit. 2017-04-28]. Dostupné z: https://en.wikipedia.org/wiki/Bisphenol_A_diglycidyl_ether#/media/File:Bisphenol_A_diglycidyl_ether_200.svg

[16] METHYL CYANOACRYLATE AND ETHYL CYANOACRYLATE. *INCHEM* [online]. c2017 [cit. 2017-05-09]. Dostupné z: http://www.inchem.org/documents/cicads/cicads/cicad36.htm#11.1

[17] By Roland Mattern - Roland1952, Public Domain, https://commons.wikimedia.org/w/index.php?curid=8343494

[18] Adhesives vs Fasteners. *Henkel Adhesives* [online]. Henkel Adhesives North America, c2017 [cit. 2017-05-14]. Dostupné z: http://na.henkel-adhesives.com/industrial/adhesives-vs-fasteners-24525.htm#b

[19] Mittal, K. L., "Adhesion Measurement: Recent Progress, Unsolved Problems, and Prospects," *Adhesion Measurement of Thin Films, Thick Films, and Bulk Coatings, ASTM STP 640, K. L.* Mittal, Ed., American Society for Testing and Materials, Philadelphia

[20] SILVA, Lucas Filipe Martins da, Andreas. ÖCHSNER a Robert D. ADAMS. *Handbook of adhesion technology*. Heidelberg: Springer, c2011. ISBN 9783642011702.

[21] OZAWA, Kenichi a Kazuhiko MASE. Evidence for chemical bond formation at rubber-brass interface: Photoelectron spectroscopy study of bonding interaction between copper sulfide and model molecules of natural rubber. *Surface Science*. 2016, **2016**(654), 14-19.

[22] Payne, A.R. (1962a). The dynamic properties of carbon black-loaded natural rubber vulcanizates: Part I. *J. Appl. Polymer Sci. 6*(19), 57–63.

[23] LARSON, Ronald G. *The structure and rheology of complex fluids*. New York: Oxford University Press, 1999. Topics in chemical engineering (Oxford University Press). ISBN 019512197X.

[24] Flocculation kinetics in the light of jamming physics: New insights into the Payne-effect in filled rubbers. *Constitutive Models For Rubber VI*. 1. London: CRC Press/Balkema, 2010, s. 205-210. ISBN 978-0-415-56327-7.

[25] Payne Effect Rubber Testing. In: *YouTube* [online]. Colimbia City: MonTechUSA, 2014 [cit. 2017-01-03]. Dostupné z: https://www.youtube.com/watch?v=vWfhKCY0htA

[26] RADZISZEWSKI, P. The steel wheel abrasion test (SWAT): A tool to study wear, friction and ore breakage in the mining industry. *WEAR*. 2009, **2009**(267), 92-98.

[27] MALÁČ, Jiří. *Gumárenská technologie: 7 zkoušky*. Zlín, 2012. Dostupné také z: http://www.utb.cz/file/36219

[28] HOOKE, Robert. *Lectures De potentia restitutiva*. London: Printed for J. Martyn, 1678.

[29] ASTM D429 - Rubber to Metal Adhesion Test Equipment. *TestResources* [online]. 2016 [cit. 09-12-2016]. Dostupné z: http://www.testresources.net/applications/standards/astm/astm-d429-rubber-to-metal-adhesion-tests

[30] LACOMBE, Robert. *Adhesion measurement methods: theory and practice*. Boca Raton, FL: CRC/Taylor, 2006. ISBN 08-247-5361-5.

[31] WILLIAMS, John A. a James J. KAUZLARICH. The influence of peel angle on the mechanics of peeling flexible adherends with arbitrary load–extension characteristics. *Tribology International*. 2005, (38), 951–958.

[32] DIANI, Julie. A review on the Mullins effect. *European Polymer Journal*. 2008, **2009**(45), 601-612.

[33] Simo JC. On a fully three-dimensional finite-strain viscoelastic damage model: Formulation and computational aspects. Comput Methods Appl Mech Engrg 1987;60:153–73.

[34] Kachanov LM. Time of the rupture process under creep conditions. Izvestiya Akad Nauk SSR Otd Tekh Nauk 1958;58:26–31.

[35] Rebound energy approach to evaluate rubber unloading-reloading process for industrial products with residual strain. LUO, R.K. a W.J. MORTEL. *Constitutive Models for Rubber IX*. 1. London: Taylor & Francis Group, 2015, s. 473-5478. ISBN 978-1-138-02873-9.

[36] Experimental investigation of anisotropy of the mechanical properties of reinforced elastomeric nanocomposites. SHARDIN, V.V., K.A. MOKHIREVA, L.A. KOMAR a A.Yu BELAJEV. *Constitutive Models for Rubber IX*. 1. London: Taylor & Francis Group, 2015, s. 495-500. ISBN 978-1-138-02873-9.

[37] R. S. Rivlin and A. G.Thomas, J. Polym. Sci. 10 (1953) 291.

[38] Mullins, L.: Effect on stretching on the properties of rubber. Journal of Rubber research 16 (1947) 275-289

[39] Mullins, L.: Theoretical model for the elastic behavior of filler-reinforced vulcanized rubbers. Rubber Chemistry and Technology 30 (1957) 551–571

[40] Mars, W. V., Fatemi, A. : Observation of the constitutive response and characterization of filled natural rubber under monotonic and cyclic multiaxial stress states. Journal of Engineering Materials and technology 126 (1) (2004) 19–28

[41] Mars, W. V., Isasi, M., Arriaga, A.: Loss of stiffness during fatigue and the development of crack precursors. Proceedings of the 8th European Conference on Constitutive Models for Rubbers (ECCMR VIII), San Sebastian (2013) 355–360

[42] Gent, A. N., Lindley,P. B., Thomas, A. G.: Cut growth and fatigue of rubbers. I. The relationship between cut growth and fatigue. Journal of Applied Polymer Science (1964) 455–466

[43] Lake, G. J., Lindley, P. B.: The mechanical fatigue limit for rubber. Journal of Applied Polymer Science 9 (1965) 1233–1251.

[44] P. Paris, F. Erdogan. A critical analysis of crack propagation laws. Journal of Basic Engineering, Transactions of the American Society of Mechanical Engineers (1963) 528–534

[45] Eisele, U., Kelbch, S.A., Engels, H.-W, 1992, The Tear Analyzer – A New Tool for Quantitative Measurements of the Dynamic Crack Growth of Elastomers, Kautschuk-Gummi- Kunststoffe, 45, pp. 1064-1069.

[46] Stoček, R.; Heinrich, G. Gehde, M., Kipscholl, R.:Analysis of Dynamic Crack Propagation in Elastomers by Simultaneous Tensile- and Pure-Shear-Mode TestingIn: W. Grellmann et al. (Eds.): Fracture Mechanics & Statistical Mech., LNACM 70, pp. 269-300

LIST OF ABBREVIATIONS

TBU	Tomas Bata University
e.g	For example
ASAP	As soon as possible
°C	Degree of centigrade
phr	Parts per hundred parts of rubber
IIR	Isoprene-isobutylene rubber
PUR	polyurethane
1K	One component system
2K	Two component system
MW	Molecular weight
etc.	et cetera
ASTM	American society for testing and materials
S_n	Sulphur bridge
CuS	Copper Sulphide
Cu_2O	Copper Oxide
ZnO	Zinc Oxide
τ	Total stress tensor
X	Hydrodynamic reinforcement
σ_m	Viscoelastic stress
σ_f^{net}	Attractive interactions
φ	Volume fraction
A	Stress-shape coefficient
ln	Natural logarithm
r	Aspect ratio

l	Particle length
d	Particle diameter
G´	Storage modulus
kPa	Kilo Pascal
CB	Carbon black
xWAT	Material abrasion test
T	Torque
µN	Load
r	Radius
rps	Revolutions per second
mm	Metric millimeter
rpm	Revolutions per minute
NR	Natural rubber
g	grams
MDR	Moving die rheometer
T_{90}	Time needed to create 90 % of Sulphur bridges
dNm	Deci Newtonmeter
T_{50}	Time needed to create 50 % of Sulphur bridges
T_{10}	Time needed to create 10 % of Sulphur bridges
t	temperature
T_{scorch}	Time of safe ending
g/ cm^3	Gram per cubic centimeter
ISO	International organization for standardization
mm/min	Millimeter per minute
σ	stress
E	Young modulus

ε	Relative prolongation
L	Actual length
L_0	Original length
kN	kilo Newton
MPa	Mega Pascal
spec	Specimen
σ_{max}	Maximum stress
ε_{max}	Maximum prolongation
M50	Modulus at 50 % prolongation
M100	Modulus at 100 % prolongation
M200	Modulus at 200 % prolongation
M300	Modulus at 300 % prolongation
AVG	Average value
SD	Standard deviation
HQG	High quality glue
LQG	Low quality glue
R	Cohesion
F	Loading force
b	Width
λ	Prolongation
φ	Peeling angle
W	Strain energy
t_0	thickness
TFA	Tear and fatigue analyzer
N	Newton

W(F) or W	Strain energy
1-d	Reduction factor
$W_0(F)$	Resting strain energy
$W_I(I)$	deviatory part of the strain energy density
$W_J(J_{el})$	volumetric part of the strain energy density
I	Invariant
C_{ij} or D_i	Material constant
W_{20}	Strain energy at 20 % prolongation peak
W_{40}	Strain energy at 40 % prolongation peak
W_{60}	Strain energy at 60 % prolongation peak
W_{80}	Strain energy at 80 % prolongation peak
W_{100}	Strain energy at 100 % prolongation peak
T	Tearing energy
A	area of crack
FCG	Fatigue crack growth
da/dn	Fatigue crack growth rate
r	Constant fatigue crack growth rate
SENT	Single edge notched tension
PS	Pure shear
Hz	Hertz
CCD	Charge coupled device
J/m^2	Joule per square meter
FEM	Finite element method

LIST OF FIGURES

Figure 1 – Example of degreasing effect [3] 11
Figure 2 – Approximate demonstration of blasting mechanism [5] 13
Figure 3 – Phosphate coating setup [9] 15
Figure 4 – Zinc coating procedure demonstration [11] 16
Figure 5 – Example of IIR monomer unit [12] 18
Figure 6 – Chemical reaction resulting in monomer [12] 18
Figure 7 – Diglycid ether of bisphenol A [15] 20
Figure 8 – polymerization of methyl-2-cyanoacrylate [17] 20
Figure 9 – Basic type of fracture 21
Figure 10 – Approximate mechanical adhesion 23
Figure 11 – Approximate structure of glued bond 25
Figure 12 – Vulcanized bond structure 27
Figure 13 – Typical example of the Payne effect test result 29
Figure 14 – Forces on the abrasion wheel [26] 30
Figure 15 – MDR3000 result at 150 °C 33
Figure 16 – Dumbbell test specimen, type 2 35
Figure 17 – Testometric M500 36
Figure 18 – Tensile test average curve 38
Figure 19 – Cohesive fracture of rubber (treated, tempered both, HQG) 39
Figure 20 – Combined fracture (treated, tempered rubber, HQG) 39
Figure 21 – Combined fracture (treated, tempered both, LQG) 39
Figure 22 – Cohesive fracture of glue (treated, tempered both, LQG) 39
Figure 23 – Peel test setup [29] 40
Figure 24 – Peel test result UP_90/10 43
Figure 25 – Rubber softening 46
Figure 26 – Schematic visualization of cyclic dynamic loading 47
Figure 27 – Double logarithmic plot of FCG rate, da/dn vs. tearing energy, T for rubber material [43] 49
Figure 28 – Photo of Tear and Fatigue Analyzer – the version of 3 electro drives 50
Figure 29 – Assembly's description 51
Figure 30 – Assembly in process 51
Figure 31 – FCG curves for rubber metal part. 52

Figure 32 – Approximate FEM model of the first cycle deformation 53
Figure 33 – Approximate FEM model of the created bond 54

LIST OF TABLES

Table 1 – Reactivity degree of the end groups in PUR [12] 19
Table 2 – Material composition 32
Table 3 – MDR3000 results 34
Table 4 – Tensile test numerical review 37
Table 5 – Peel test numerical review 42
Table 6 – Energy loss due to rubber softening 45